

Review

# Recent Progress in the Use of SnO<sub>2</sub> Quantum Dots: From Synthesis to Photocatalytic Applications

Babu Bathula <sup>1,\*</sup> , Thirumala Rao Gurugubelli <sup>2</sup>, Jihyung Yoo <sup>3</sup> and Kisoo Yoo <sup>1,\*</sup><sup>1</sup> School of Mechanical Engineering, Yeungnam University, Gyeongsan 38541, Republic of Korea<sup>2</sup> Physics Division, Department of Basic Sciences and Humanities, GMR Institute of Technology, GMR Nagar, Rajam 532127, India; thirumala.phy@gmail.com<sup>3</sup> Department of Automotive Engineering, Hanyang University, Seoul 04763, Republic of Korea; jihyungyoo@hanyang.ac.kr

\* Correspondence: babu.physicist@gmail.com (B.B.); kisooyoo@yu.ac.kr (K.Y.)

**Abstract:** This review article provides current developments in SnO<sub>2</sub> quantum dots (QDs) as effective catalysts over the last five years. SnO<sub>2</sub> QDs are exceptional prospects for catalytic applications because of their high surface area, compact size, and tunable optical features. SnO<sub>2</sub> QDs have recently made strides in their production and functionalization, which has enabled successful use of them as photocatalytic catalysts. The basic concepts of SnO<sub>2</sub> QDs, including their electrical and optical characteristics, are described in this review paper, along with the most current findings on their production and functionalization. Additionally, it covers the fundamental mechanisms that support SnO<sub>2</sub> QDs' catalytic activity and emphasizes the difficulties involved in using them as catalysts. Lastly, it offers a forecast for the direction of research in this quickly evolving topic. Overall, our analysis demonstrates SnO<sub>2</sub> QDs' potential as a successful and cutting-edge catalytic system in recent years.

**Keywords:** SnO<sub>2</sub>; QDs; synthesis; heterojunction; photocatalysis; dye degradation



**Citation:** Bathula, B.; Gurugubelli, T.R.; Yoo, J.; Yoo, K. Recent Progress in the Use of SnO<sub>2</sub> Quantum Dots: From Synthesis to Photocatalytic Applications. *Catalysts* **2023**, *13*, 765. <https://doi.org/10.3390/catal13040765>

Academic Editors: Amr Fouda and Mohammed F. Hamza

Received: 11 March 2023

Revised: 14 April 2023

Accepted: 16 April 2023

Published: 17 April 2023



**Copyright:** © 2023 by the authors. Licensee MDPI, Basel, Switzerland. This article is an open access article distributed under the terms and conditions of the Creative Commons Attribution (CC BY) license (<https://creativecommons.org/licenses/by/4.0/>).

## 1. Introduction

Water pollution is a major issue for modern society, caused by the discharge of untreated waste into water sources [1]. This contamination can cause health problems, ecological damage, and economic losses. Quantum dots (QDs) are semiconductor crystals with sizes ranging from 1 to 10 nanometers in diameter. Owing to their small size and distinctive physical and chemical characteristics, QDs are appealing for a variety of applications [2]. Several materials, including semiconductor, metal, and carbon QDs, can be used to create QDs. Because of their remarkable optical and electrical capabilities, semiconductor QDs have been the subject of most research [3]. For example, II–VI and III–V compounds with high quantum yield, narrow emission spectra, and high charge carrier mobility, such as CdSe, CdTe, InP, and GaAs, have received a great deal of attention [4]. Due to their distinctive qualities and possible uses, metal oxide QDs, such as SnO<sub>2</sub>, TiO<sub>2</sub>, and ZnO, have also received a lot of attention [5]. The huge surface area of metal oxide QDs, which enables effective catalytic reactions, is one of their key advantages. SnO<sub>2</sub> QDs, in particular, have a number of distinctive qualities that set them apart from other QD kinds. First off, SnO<sub>2</sub> is an environmentally beneficial substitute for other harmful or expensive materials because it is a substance that is readily available on Earth and is not toxic [6]. Second, SnO<sub>2</sub> QDs are promising candidates for a variety of applications, including photocatalysis, sensing, and energy conversion, thanks to their superior optical and electrical characteristics, which include a high surface area, strong stability, and a broad bandgap [7].

Furthermore, SnO<sub>2</sub> QDs have demonstrated strong catalytic activity in the oxidation of organic contaminants and the water-splitting process that produces hydrogen [8]. This is a result of their special electrical characteristics, which enable effective charge separation and

transfer. These characteristics include high electron mobility and an appropriate conduction band location [9]. SnO<sub>2</sub> QDs' tiny size and the large surface area also make more active sites for catalytic reactions possible, improving the efficiency of such reactions. Many techniques for regulating SnO<sub>2</sub> QDs' size, shape, and surface properties have been developed as a result of in-depth research into their synthesis and functionalization [10]. This has created new possibilities for modifying SnO<sub>2</sub> QDs' catalytic performance for certain applications. More study is required to completely comprehend their underlying mechanisms and improve their catalytic efficiency, given the intriguing features and possible uses of SnO<sub>2</sub> QDs. In order to accomplish this, new synthesis and functionalization techniques must be created, and the relationship between a substance's structure, characteristics, and performance must be better understood. These investigations have demonstrated that SnO<sub>2</sub> QDs may degrade a variety of pollutants. Furthermore, they have demonstrated effectiveness in disinfecting water sources by inactivating pathogenic bacteria and viruses. Additionally, SnO<sub>2</sub> QDs can be easily modified and functionalized to enhance their performance in water treatment [11]. As the size of the SnO<sub>2</sub> QDs decreases, the bandgap energy increases, which leads to enhanced light absorption and higher photocatalytic activity. This unique characteristic makes SnO<sub>2</sub> QDs more effective photocatalysts than bulk SnO<sub>2</sub> [6]. SnO<sub>2</sub> QDs exhibit enhanced reactivity compared to bulk SnO<sub>2</sub> due to their high surface energy and the presence of surface defects. These characteristics make it easier for reactive oxygen species (ROS) to develop, including hydroxyl radicals (•OH), which are in charge of degrading contaminants [12]. The bandgap energy of SnO<sub>2</sub> QDs can be adjusted by controlling their size and surface chemistry. This property enables the optimization of the photocatalytic activity of SnO<sub>2</sub> QDs for specific applications, such as the degradation of particular pollutants or the production of hydrogen through water splitting [13]. SnO<sub>2</sub> QDs display excellent stability under different environmental conditions, making them suitable for long-term water treatment applications [14].

This article will focus on the optical and electronic characteristics of SnO<sub>2</sub> QDs that are relevant to photocatalysis. The optical properties of SnO<sub>2</sub> QDs are size-dependent and result from the quantum confinement phenomenon [15]. The energy levels within QDs are discrete, and the bandgap energy increases as the particle size decreases. Consequently, SnO<sub>2</sub> QDs have a tunable bandgap that can be customized by altering their size. These QDs have an optical absorption edge that reaches into the visible range, allowing them to be utilized for visible light photocatalysis [16]. Furthermore, SnO<sub>2</sub> QDs exhibit strong light scattering and luminescence, which can enhance photocatalytic efficiency. With respect to electronic properties, SnO<sub>2</sub> QDs have a high surface area to volume ratio, resulting in an increased number of surface defects and trap states [8]. The photocatalytic effectiveness of the QDs may decrease as a result of these defects and trap states acting as recombination foci for photogenerated electron–hole pairs. The electrical characteristics of SnO<sub>2</sub> QDs can be changed by adding surface changes or doping to overcome this restriction [10]. For instance, SnO<sub>2</sub> QDs that have been modified with other materials, such as TiO<sub>2</sub>, have demonstrated improved electron extraction and transport properties as well as suppressed charge recombination, resulting in better photocatalytic performance [17]. Additionally, doping SnO<sub>2</sub> QDs with nitrogen or carbon can introduce new energy levels that can act as electron traps, reducing the recombination rate and increasing the photocatalytic activity [18]. SnO<sub>2</sub> QDs can be synthesized utilizing a variety of methods, including the hydrothermal method, solvothermal method, and sol–gel method [19]. They have demonstrated great potential as a solution to water pollution, and this review aims to provide an in-depth analysis of recent advances in SnO<sub>2</sub> quantum dot synthesis, modification, and application in water treatment. To encourage the wider deployment of SnO<sub>2</sub> QDs for environmental applications, this review will emphasize major discoveries, problems, and prospects for future research in this area.

The size-dependent optical characteristics of SnO<sub>2</sub> QDs are ascribed to the quantum confinement effect [20]. The energy levels in the QDs are discrete, and the bandgap energy increases with decreasing particle size. As a result, SnO<sub>2</sub> QDs have a tunable bandgap

that can be tailored by controlling their size. SnO<sub>2</sub> QDs have been shown to possess a remarkable light-harvesting capacity, thereby enhancing photocatalytic efficiency. Additionally, the high surface area to volume ratio of SnO<sub>2</sub> QDs has been found to contribute to improved photocatalytic performance. This can be improved by modifying their electronic properties through surface modifications or doping. Strategies, such as doping, composite construction, and adjustment of co-catalyst size, can be employed to improve the photocatalytic performance of SnO<sub>2</sub> QDs [21]. Ultimately, the information in this review will give readers an understanding of the potential of SnO<sub>2</sub> QDs as a water pollution remedy and the methods for improving their photocatalytic performance for environmental applications. In recent years, there has been a lot of interest in the usage of nanocomposites of SnO<sub>2</sub> QDs with other semiconductors to enhance photocatalytic performance. Over the past 5 years, multiple research articles have focused on the importance of making these nanocomposites to create heterostructure formations that improve photocatalytic activity. In order to create nanocomposites and heterostructure composites with improved photocatalytic activity for water treatment and other applications, these investigations looked into several ways to combine SnO<sub>2</sub> with other semiconductors [22–24]. The higher visible light absorption and effective separation of photogenerated electron–hole pairs at the nanocomposite interface are two reasons for the enhanced photocatalytic activity of these materials. The authors also reported a synergistic effect between the SnO<sub>2</sub> QDs and other selected components in the nanocomposite, which improved the visible light absorption and the separation of photogenerated electron–hole pairs in the heterojunctions. Overall, the studies on nanocomposites of SnO<sub>2</sub> QDs with other semiconductors have demonstrated promising results for enhancing photocatalytic activity. These findings could have important implications for developing more efficient and sustainable technologies for water treatment and other applications.

## 2. Synthesis Protocols

SnO<sub>2</sub> QDs are prepared through various methods, such as solution synthesis, hydrothermal synthesis, and chemical reduction synthesis, among others [25–29]. While each approach has benefits and drawbacks, the choice of synthesis process is dictated by the desired QD qualities and the particular application. Alternative techniques for creating SnO<sub>2</sub> QDs include sonochemical synthesis, microwave-assisted synthesis, solvothermal synthesis, and template-assisted synthesis, among others [30]. Understanding the SnO<sub>2</sub> QD synthesis methods is crucial since the synthesis process can affect the QDs' characteristics and performance, which can affect their potential usage in a variety of applications, such as photocatalysis. SnO<sub>2</sub> QDs can have their size, shape, and crystal structure controlled throughout the fabrication process, which may have an effect on how well they function as photocatalysts. Thus, the advancement of SnO<sub>2</sub> QD applications in areas including water purification, air purification, and solar energy conversion depends on the development of effective and controllable synthesis methods [31]. To improve the synthesis techniques for SnO<sub>2</sub> QDs and to comprehend the underlying mechanisms that control their characteristics and performance, more research is required.

### 2.1. Microwave-Assisted Synthesis

In order to create SnO<sub>2</sub> QDs, microwave-assisted synthesis is a practical and efficient method. This technique has the advantage of producing uniformly sized, high-quality QDs in a short period of time. Inducing the creation of nuclei and accelerating particle growth using microwave irradiation can lead to the formation of well-defined, extremely uniform SnO<sub>2</sub> QDs [32]. This method offers a highly precise, scalable, and energy-efficient method for producing SnO<sub>2</sub> QDs. Furthermore, microwave-assisted synthesis is a low-temperature technique that uses less energy and produces fewer undesirable byproducts. This process is simple and affordable, making it simple to scale up for the large-scale manufacturing of SnO<sub>2</sub> QDs. For creating SnO<sub>2</sub> QDs, microwave-assisted synthesis has a number of benefits [33]. Microwave irradiation, which accelerates particle growth, can make it easier

to produce SnO<sub>2</sub> QDs with precise size and shape. This method is also very adaptable and may be used to make vast amounts of SnO<sub>2</sub> QDs. This process is appealing for the mass production of SnO<sub>2</sub> QDs since it is simple, affordable, and energy-efficient. This method was used by researchers Xu et al. to produce densely packed, extremely crystalline SnO<sub>2</sub> QDs [26]. Smaller than the SnO<sub>2</sub> Bohr radius, they were able to produce homogenous particles with an average radius of 1–1.5 nm. This raises the possibility of a substantial quantum-size effect, in which a dot's wave function extends into that of its neighbors, resulting in an electrically active QD solid. According to these results, the distinctive properties of SnO<sub>2</sub> QDs and their potential applications in several fields are now well characterized [26,32,33].

Geng et al. also employed a microwave-assisted method to synthesize SnO<sub>2</sub> QDs [32]. Their technique involved adding tin (II) chloride dehydrate to a mixed solvent of ethanol and water, which was then subjected to microwave irradiation at 180 °C for 30 min. The resulting SnO<sub>2</sub> QDs had an average size of 4–6 nm and a consistent spherical shape. This method allowed for a shorter reaction time and higher yield compared to conventional hydrothermal methods. Additionally, the smaller particle size of the SnO<sub>2</sub> QDs obtained through microwave-assisted synthesis is advantageous for higher surface area and improved electrochemical performance. Parthibavarman et al. employed a similar strategy but different precursor materials to create SnO<sub>2</sub> QDs [33]. They were successful in producing particles with a narrow size range and a mean diameter of 2.8 nm. When exposed to visible light, these particles demonstrated remarkable photocatalytic activity in degrading rhodamine B. High-quality SnO<sub>2</sub> QDs with features that could make them helpful in a variety of applications, from electronics to photocatalysis, are being produced successfully by using microwave-assisted synthesis.

## 2.2. Hydrothermal Synthesis

Hydrothermal synthesis is a promising technique for synthesizing SnO<sub>2</sub> QDs due to its several advantages. It provides precise control over particle size and morphology by adjusting reaction conditions such as temperature, pressure, and reaction time. This control over the particle size and shape is crucial as it directly affects the properties and performance of the QDs. Additionally, hydrothermal synthesis leads to high-quality SnO<sub>2</sub> QDs with a high degree of crystallinity, purity, and uniformity due to the high-temperature and high-pressure conditions that promote the growth of single crystals and reduce the formation of impurities. Moreover, hydrothermal synthesis provides a somewhat easy and affordable way to produce SnO<sub>2</sub> QDs on a large scale. Recent research studies have also shown the effectiveness of hydrothermal synthesis in the preparation of SnO<sub>2</sub> QDs. For instance, Praveen et al. utilized hydrothermal synthesis to prepare SnO<sub>2</sub> QDs for use in photodetectors [25], while Yu et al. synthesized SnO<sub>2</sub> QDs by varying the concentration of C<sub>2</sub>H<sub>3</sub>ClO<sub>2</sub> to enhance their photocatalytic activity (Figure 1) [34]. Overall, the production of high-quality and tightly controlled SnO<sub>2</sub> QDs using a straightforward and scalable procedure is made possible by hydrothermal synthesis.

## 2.3. Wet Chemical Synthesis

Solution-based synthesis is a highly popular method for creating colloidal SnO<sub>2</sub> QDs due to its ability to produce uniform particles with controlled size and shape [27]. The most often used method involves injecting a heated organic solvent containing a capping agent with a precursor solution of SnCl<sub>4</sub> and a reducing agent. The capping agent stabilizes the nanoparticles and prevents agglomeration, while the organic solvent serves as a reaction medium. Since the reaction is commonly conducted at high temperatures, SnO<sub>2</sub> QDs with a restricted size distribution can form quickly and expand rapidly. The quality of the colloidal QDs can be improved by adding further purification procedures such as centrifugation and solvent washing. With the help of this technique, colloidal SnO<sub>2</sub> QDs with customized properties can be made in a variety of applications, such as sensing, solar cells, and catalysis.

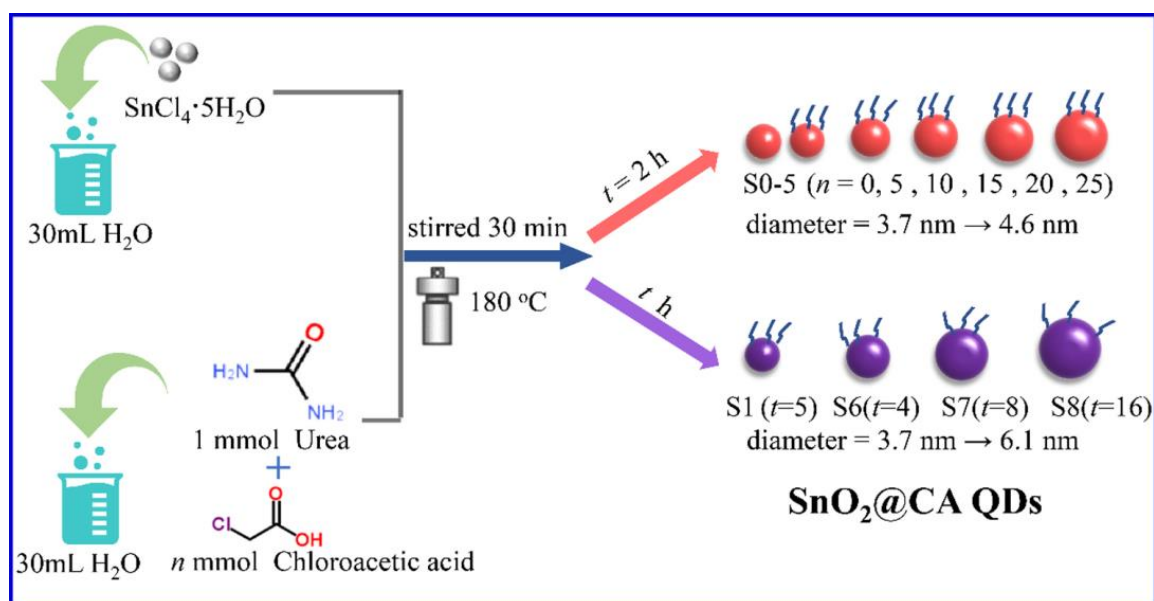


**Figure 1.** Diagrammatic representation of the  $\text{SnO}_2$  QD synthesis process [34], Copyright 2021, Elsevier.

Liu et al. employed a straightforward solution processing approach to convert  $\text{SnCl}_2 \cdot 2\text{H}_2\text{O}$  into a  $\text{SnO}_2$  QD colloidal solution, with anhydrous ethanol and deionized water serving as the solvent [35]. Then, for 48 h, the suspension was constantly stirred to create a  $\text{SnO}_2$  colloidal precursor solution. The use of this solution as an electron transport layer led to increased electron extraction, reduced charge recombination, and dramatically improved total solar cell efficiency. By dispersing  $\text{SnCl}_2 \cdot 2\text{H}_2\text{O}$  and thiourea in DI water for one to two days, Gao et al. were able to create a colloidal solution of  $\text{SnO}_2$  QDs, which was then coupled with rGO for battery applications (Figure 2) [36]. Jin et al. also utilized a similar approach to create  $\text{SnO}_2$  QDs and functionalize  $\text{MoO}_3$  nanobelts for high-selectivity ethylene sensing [22]. Meanwhile, Chen et al. utilized  $\text{SnCl}_4 \cdot 5\text{H}_2\text{O}$ , NaOH,  $\text{H}_2\text{O}$ , and ethanol to make very stable  $\text{SnO}_2$  QDs, which were made in a Teflon-lined, stainless steel autoclave and heated at  $150^\circ\text{C}$  for 6 h [37]. They employed tetramethylammonium hydroxide in the synthesis to obtain highly stable QDs, which were used for high-performance QLEDs with a  $\text{SnO}_2$ -based ETL. Luo et al. used a different method to prepare  $\text{SnO}_2$  QDs for  $\text{NO}_2$  gas sensing [38]. They mixed  $\text{SnCl}_4 \cdot 5\text{H}_2\text{O}$ , oleylamine, oleic acid, and deionized water in a three-neck flask and subjected it to vacuum conditions at  $30^\circ\text{C}$  for an hour. After the mixture became clear and transparent, the temperature of the flask was raised to  $80^\circ\text{C}$  under an  $\text{N}_2$  gas flow for six hours. The resulting mixture was then put into autoclaves and kept there for three hours at  $180^\circ\text{C}$ . The studies mentioned above have demonstrated the potential of colloidal  $\text{SnO}_2$  QDs for various applications, including photocatalysis, electrochemical energy storage, and sensing. However, it is crucial to carefully consider the synthesis parameters, as the choice of synthesis method and reaction conditions can impact the size, morphology, and properties of the resulting QDs. In conclusion, a solution-based synthesis is a promising approach for creating colloidal  $\text{SnO}_2$  QDs with well-controlled sizes and properties.

#### 2.4. Chemical Reduction Approach

Another extensively used technique for creating  $\text{SnO}_2$  QDs is chemical reduction. In this process, a reducing agent and a stabilizing agent are utilized to reduce the precursor metal ions into the QDs. This method allows for the use of both organic and inorganic reducing agents, such as sodium borohydride and hydrazine. The size and shape of the resultant QDs might vary greatly depending on the reducing agent used. The reduction reaction produces  $\text{SnO}_2$  QDs with a limited size range when it occurs at low temperatures,

usually between 60 and 90 °C. The stabilizing agent, typically a surfactant or polymer, helps to prevent the particles from agglomerating and stabilizes the surface of the QDs. Post-synthesis purification steps, such as centrifugation and washing with solvents, can further enhance the quality of the colloidal QDs. The chemical reduction method offers a versatile and straightforward approach for preparing SnO<sub>2</sub> QDs with tailored properties, making them promising candidates for various applications, including sensing, energy storage, and catalysis (Figure 3). Dutta et al. utilized a straightforward chemical reduction method to produce SnO<sub>2</sub> QDs with SnCl<sub>4</sub>·5H<sub>2</sub>O and hydrazine hydrate as precursors [28]. The reaction was conducted at 100 °C for 18 h, yielding QDs ranging from 2 to 3 nm. Likewise, Babu et al. employed a similar method to synthesize in situ Ag/SnO<sub>2</sub> and Au/SnO<sub>2</sub> QDs for photocatalytic degradation of water pollutants, such as MO, MB, and RhB dyes [39,40].

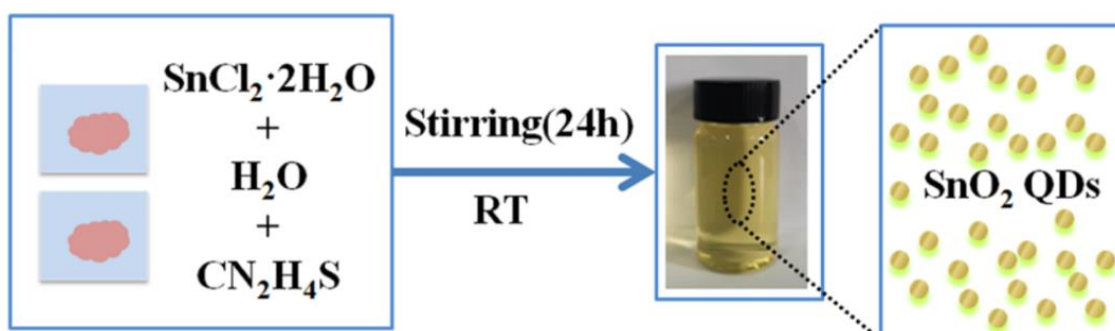


Figure 2. Colloidal synthesis of SnO<sub>2</sub> QDs [35], Copyright 2020, ACS.

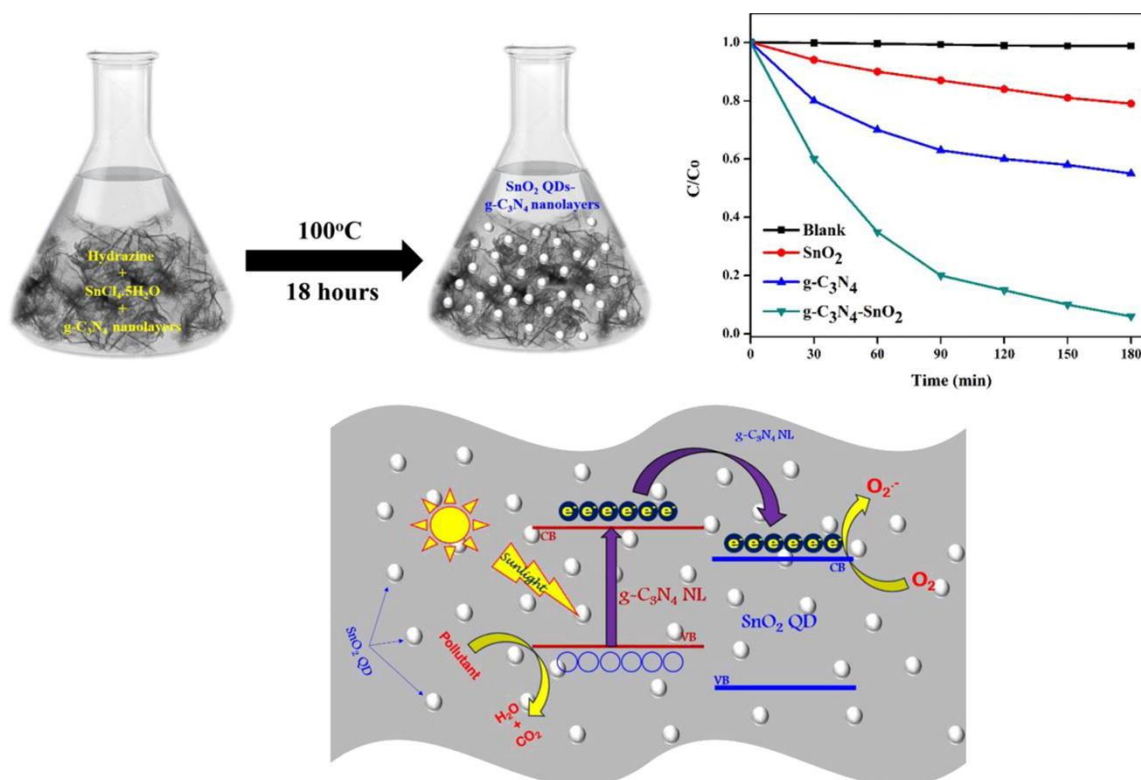


Figure 3. Synthesis and photocatalytic application of SnO<sub>2</sub> QDs [41], Copyright 2018, Elsevier.

### 2.5. Other Methods

Wahab et al. synthesized colloidal SnO<sub>2</sub> QDs via a reflux method [42]. Firstly, tin chloride was added to methanol and continuously stirred until fully dissolved. Using NH<sub>3</sub> solution, the pH was brought down to 9.5 before the mixture was transferred to a

refluxing pot with two necks and cooked at 65 °C for three hours. The generated SnO<sub>2</sub> QDs were examined for possible biological uses on cancerous myoblast (C<sub>2</sub>C<sub>12</sub>) cells. SnO<sub>2</sub> QDs were synthesized using a biosynthesis approach by Fatimah et al., in which Clitoria ternatea flower extract and SnCl<sub>2</sub>·2H<sub>2</sub>O were utilized as the tin precursor [43]. The size range of the QDs that the authors were able to obtain was 4–6 nm. The prepared SnO<sub>2</sub> QDs showed efficient degradation of the rhodamine B pollutant. Kumar et al. utilized the solution combustion method to synthesize SnO<sub>2</sub> QDs [29]. They used urea (CO(NH<sub>2</sub>)<sub>2</sub>) and tin chloride pentahydrate (SnCl<sub>4</sub>·5H<sub>2</sub>O) as precursors in DI water for their study. Urea was used as a fuel to start the reaction, and the solution was heated in a furnace to a temperature range of 350 to 550 °C. The SnO<sub>2</sub> QDs obtained through this method had a crystallite size of less than 4 nm. Similarly, Babu et al. utilized the solution combustion synthesis method to prepare various transition metal-doped SnO<sub>2</sub> QDs for photocatalytic applications [40]. Table 1 describes the synthesis techniques of SnO<sub>2</sub> QDs.

**Table 1.** SnO<sub>2</sub> quantum dot synthesis techniques.

Synthesis Approach	Sn Precursor	Processing Temperature	Reaction Time	Ref
Hydrothermal	SnCl <sub>4</sub> ·5H <sub>2</sub> O	150 °C	6 h	[37]
Hydrothermal	SnCl <sub>4</sub> ·5H <sub>2</sub> O	180 °C	2 h	[34]
Hydrothermal	SnCl <sub>2</sub>	140 °C	4 h	[25]
Hydrothermal	SnCl <sub>4</sub> ·5H <sub>2</sub> O	160 °C	8 h	[44]
Hydrothermal	SnCl <sub>2</sub> ·2H <sub>2</sub> O	160 °C	6 h	[45]
Hydrothermal	Na <sub>2</sub> SnO <sub>3</sub> ·3H <sub>2</sub> O	180 °C	24 h	[46]
Microwave	SnCl <sub>2</sub> ·2H <sub>2</sub> O	180 °C	30 min	[32]
Microwave	SnCl <sub>4</sub> ·5H <sub>2</sub> O	120 °C	15 min	[33]
Microwave	SnCl <sub>2</sub> ·2H <sub>2</sub> O	110 °C	6 h	[26]
Microwave	SnCl <sub>4</sub> ·5H <sub>2</sub> O	160 °C	20 min	[47]
Wet chemical	SnCl <sub>4</sub> ·5H <sub>2</sub> O	100 °C	18 h	[39]
Wet chemical	SnCl <sub>2</sub> ·2H <sub>2</sub> O	RT	6 h	[22]
Reflux	SnCl <sub>2</sub> ·2H <sub>2</sub> O	65 °C	3 h	[42]
Hummers	SnCl <sub>2</sub> ·2H <sub>2</sub> O	180 °C	24 h	[35]
Solution processing	SnCl <sub>2</sub> ·2H <sub>2</sub> O	RT	48 h	[27]
Solution combustion	SnCl <sub>4</sub> ·5H <sub>2</sub> O	450 °C	-	[48]
Self-assembly	SnCl <sub>2</sub> ·2H <sub>2</sub> O	RT	24 h	[11]
One pot Biosynthesis	SnCl <sub>2</sub> ·2H <sub>2</sub> O	60 °C	12 h	[43]
In situ	SnCl <sub>4</sub> ·5H <sub>2</sub> O	100 °C	18 h	[49]

### 3. Modification of SnO<sub>2</sub> QDs for Photocatalytic Applications

#### 3.1. Doping of SnO<sub>2</sub> QDs

Enhancing the photocatalytic efficiency of SnO<sub>2</sub> QDs through doping is a crucial method. Doping can inject impurity levels within the band gap, improving the characteristics of light absorption and lowering the rate at which electron–hole pairs recombine. Dopants can be included in SnO<sub>2</sub> QDs to modify the band gap energy, which can enhance photocatalytic activity in the visible light spectrum [50]. Additionally, doping can also alter the surface properties of SnO<sub>2</sub> QDs, which can enhance the surface reactivity and increase the adsorption capacity for target pollutants [51]. SnO<sub>2</sub> QDs are, therefore, a desirable material for environmental cleanup applications due to the large improvements in photocatalytic efficiency and selectivity that can be achieved through doping. The choice

of dopant elements for SnO<sub>2</sub> QDs in photocatalytic applications depends on the desired properties and specific application requirements. Generally, transition metals such as Fe, Co, Ni, Mn, and Cu, as well as non-metals, such as N and C, have been successfully used as dopants in SnO<sub>2</sub> QDs for photocatalytic applications [29,45,52,53]. SnO<sub>2</sub> QDs' electrical and optical characteristics can be changed by these dopants, improving the photocatalytic activity, charge transfer efficiency, and absorption spectrum. For example, nitrogen doping can narrow the bandgap of SnO<sub>2</sub> QDs, increasing their visible light absorption, while transition metal doping can enhance their catalytic activity toward specific reactions [54]. However, the doping concentration, kind of dopant, and manufacturing process should be carefully regulated in order to achieve the desired properties and avoid any negative effects on photocatalytic performance. Chen et al. recently created a quick and easy approach for creating Ni-doped SnO<sub>2</sub> QDs with improved photocatalytic efficiency for breaking down Rhodamine B [44]. The SnO<sub>2</sub> QDs were created using a hydrothermal technique, and the researchers then looked at how Ni doping affected the photocatalytic activity of the SnO<sub>2</sub> QDs. After 28 min of solar light irradiation, the results showed that QDs with a Ni/Sn atomic ratio of 1% had the best photocatalytic performance, destroying 91.5% of Rhodamine B. Ni was added to the SnO<sub>2</sub> QDs, which improved photodegradation performance by increasing light harvesting and reducing band gaps. SnO<sub>2</sub> QDs also offered more active sites for photocatalytic reactions due to their small particle size and high specific surface area. The 1% Ni-doped SnO<sub>2</sub> QDs outperformed their pure counterparts in terms of photocatalytic activity.

In their study, Wang et al. looked at how niobium alteration could enhance the visible-light photocatalytic abilities of SnO<sub>2</sub> QDs (Figure 4) [45]. One-step hydrothermal synthesis of niobium-modified SnO<sub>2</sub> QDs was carried out by the researchers, who then evaluated their photocatalytic capabilities. The changed band structure brought on by the presence of the transition metal was blamed for the increase in photocatalytic activity. The rate constant of Nb-SnO<sub>2</sub> QDs in MO deterioration was found to be 2.34 times higher than that of pristine SnO<sub>2</sub> QDs after characterizing the crystal structures and optical characteristics of the Nb-SnO<sub>2</sub> QDs. According to the study's findings, the changed band structure caused by the transition metal plays a significant role in increasing the photocatalytic abilities of SnO<sub>2</sub> QDs when exposed to visible light. For the breakdown of antibiotic pollutants caused by visible light, Wang et al. presented a study on the modification of tin oxide QDs' band structure and the improvement of their photocatalytic capabilities through Mo doping [45]. The effective production of extremely potent hydroxyl radicals is made possible by the photogenerated holes' strong oxidizing properties in the valence band edge over 3 eV. This study explores the impact of Mo inclusion on the microstructural, compositional, electrical, and optical properties of SnO<sub>2</sub> QDs and describes a method for producing them. The modified QDs demonstrated antibiotic elimination capabilities via visible-light-driven photocatalysis. Mo-doped SnO<sub>2</sub> QDs were easily synthesized by the authors utilizing a green synthesis technique. Mo dopants changed the electrical band structure of SnO<sub>2</sub> QDs, lowering the band gap and bringing about photocatalytic functions controlled by visible light. With a degradation efficiency of up to 96.5%, the nanostructured photocatalysts showed effective capabilities in the tetracycline hydrochloride degradation process. In a study, Chu et al. looked at how well SnO<sub>2</sub> QDs doped with Bi<sup>3+</sup> worked in combination with BiPO<sub>4</sub> to clean various organic contaminants [46]. The synthetic composite material successfully broke down a number of organic dyes and medicines. In this article, a broad-spectrum photocatalyst called BiPO<sub>4</sub>/Bi-SnO<sub>2</sub> QD is synthesized in detail, and its enhanced photocatalytic performance in comparison to pure Bi-SnO<sub>2</sub> and BiPO<sub>4</sub> is investigated. The composite material was created by a simple hydrothermal one-pot process and demonstrated enhanced photocatalytic efficacy when exposed to artificial sunlight. The effects of catalyst dosage, starting concentration, and common anions were all studied in relation to the breakdown of bisphenol A (BPA). The composite material also showed success in degrading a number of organic dyes and medicines.

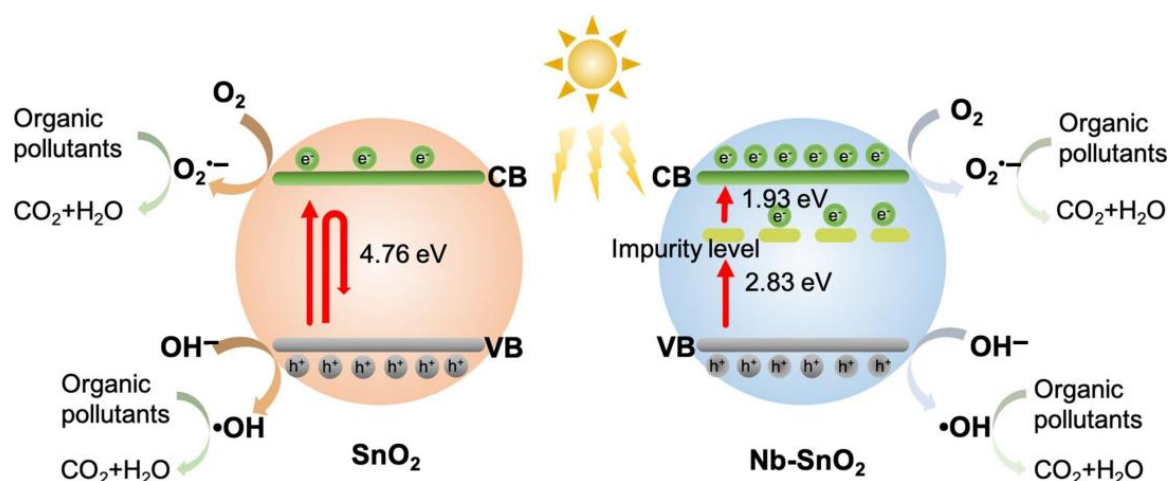


**Figure 4.** Photocatalytic mechanism of pure SnO<sub>2</sub> QDs and Nb-SnO<sub>2</sub> QDs [45], Copyright 2022, Elsevier.

High photocatalytic activity of pure and Ag-doped SnO<sub>2</sub> QDs produced using a one-step microwave-assisted technique was reported by Parthibavarman et al. The optical characteristics of SnO<sub>2</sub> were greatly enhanced by Ag doping [33]. Under visible light irradiation, the Ag-doped SnO<sub>2</sub> catalyst demonstrated a maximum RhB degrading efficiency of 97.5% with good reusability and stability after seven cycles. SnO<sub>2</sub> nanoparticles' structural, morphological, compositional, and optical characteristics, as well as their photocatalytic performance, were all influenced by the amount of Ag dopant present. With Ag doping, SnO<sub>2</sub>'s band gap was reduced from 3.54 to 3.09 eV. According to a study by Shao et al., Nb-modified SnO<sub>2</sub> QDs produced through aqueous synthesis were used to clean agricultural waste in situ while also photocatalyzing the breakdown of polyethylene [36]. According to the study, Nb-modified SnO<sub>2</sub> QDs can be used to remove polyethylene in an innovative and environmentally benign way. After 6 h of exposure to visible light, Nb-SnO<sub>2</sub> QDs had a 29% degradation efficiency. Due to the effective photocatalytic degradation occurring in visible light, this low-cost technology offers a fresh approach to the in situ treatment of agricultural waste, and their potential for real-world use is highlighted. Babu et al. studied the improved visible light photocatalytic activity of solution combustion-synthesized Cu-doped SnO<sub>2</sub> QDs [40]. In this study, solution combustion synthesis was successfully used to create Cu-doped SnO<sub>2</sub> QDs and the photocatalytic degradation of the methyl orange dye under visible light irradiation was examined. The findings demonstrated that the optical band gap energy of the QDs decreased with increasing Cu content. The best photocatalytic performance was demonstrated by the QDs doped with 0.03 mol% Cu, which degraded the methyl orange dye by 99% under visible light in about 180 min. These results point to the potential of solution combustion-produced Cu-doped SnO<sub>2</sub> QDs as efficient photocatalysts for the degradation of organic impurities when exposed to visible light.

### 3.2. SnO<sub>2</sub> QDs' Decorated 1D Nanostructures

Due to their distinct optical and electrical characteristics, one-dimensional core-shell nanorods are a potential material for photocatalytic applications. Efficient charge separation is facilitated by the core-shell structure, which is essential for high photocatalytic performance. The nanorods' high aspect ratio and anisotropic shape provide a large surface area and directional charge transfer, respectively, which are beneficial for catalytic reactions. Core-shell nanorods can be made from a variety of substances, including metal oxides and semiconductors, and they can be customized for particular applications by varying the size and makeup of the core and shell. The application of QDs as a shell material is one fascinating field of research. For example, SnO<sub>2</sub> QDs as the shell material in core-shell nanorods enhance their performance. SnO<sub>2</sub> QDs have unique electronic and optical properties that allow efficient charge separation, and their anisotropic shape facilitates directional charge

transfer, which enhances photocatalytic activity. Various methods, including hydrothermal synthesis and sol–gel methods, can be used to synthesize core–shell nanorods with SnO<sub>2</sub> QDs as the shell material [55]. The potential applications of 1-dimensional core-shell nanorods with SnO<sub>2</sub> QDs as the shell material are significant and include environmental remediation and energy production.

The increased photoelectrochemical performance of cadmium sulfide–tin oxide QD core–shell nanorods was examined in a study by Babu et al. [56]. Using hydrothermal synthesis and straightforward chemical synthesis, core–shell nanorods with a cadmium sulfide core and a tin oxide quantum dot shell were created. The researchers found that the core–shell nanorods' photoelectrochemical performance outperformed that of pure cadmium sulfide nanorods. This increase was due to the tin oxide quantum dot shells' effective lowering of the core–shell nanorods' bandgap from 2.37 eV to 2.35 eV, which led to larger photocurrents and lower charge transfer resistance. Overall, the research shows that core–shell nanorods with tin oxide QDs are a viable material for photoelectrochemical applications that are driven by solar light.

Babu et al. looked into optimizing core–shell nanostructures to improve the photocatalytic activity of colloidal SnO<sub>2</sub> QD-decorated CdS NRs with visible light (Figure 5a) [40]. It was revealed that the colloidal SnO<sub>2</sub> QDs' synergistic effect helped these nanorods perform better in the dye degradation process. This paper describes a novel two-step method for creating core–shell heterojunction photocatalysts for SnO<sub>2</sub> QDs using hydrothermal and ultrasonication procedures. Colloidal SnO<sub>2</sub> QDs were used to completely decorate the exterior of the CdS NRs that were created, with the quantity chosen to maximize degrading efficiency. The colloidal SnO<sub>2</sub> QDs protected the CdS NRs' surface and helped explain the NRs' superior dye-degradation performance (Figure 5b). These findings show that CdS@SnO<sub>2</sub> core–shell NRs have the potential to be an effective material for photocatalytic processes involving visible light. The visible-light photocatalytic performance of CdS@SnO<sub>2</sub> nanorods for the selective oxidation of benzyl alcohol to benzaldehyde was the focus of Liu et al. studies [51]. The core–shell structure of the nanorods was found to effectively accelerate the separation rate of electron–hole pairs and the electron lifetime of CdS nanorods, increasing visible light absorption and improving photocatalytic activity. Utilizing the use of a solvent-assisted interfacial reaction technique and ultrasonic stirring to anchor SnO<sub>2</sub> nanoparticles to the surface of CdS NRs, the scientists created the core–shell structure CdS@SnO<sub>2</sub> nanorods. The photocatalytic activity of the nanorods for the selective oxidation of benzyl alcohol to benzaldehyde under visible light irradiation was shown to be greatly improved by the core–shell configuration. This improvement was attributed to the core–shell structure's improved visible light absorption, increased surface area, and more effective electron and hole separation.

Lee et al. have described the extremely effective interfacial charge transfer-based photocatalytic performance of SnO<sub>2</sub>-deposited ZnS nanorods [57]. The higher separation rate of photogenerated charges is principally responsible for the increased photocatalytic degradation efficiency of SnO<sub>2</sub>/ZnS nanocomposites. In this study, SnO<sub>2</sub>/ZnS nanocomposites with improved photocatalytic activity and photostability are made using a two-step hydrothermal procedure assisted by hydrazine. In comparison to pristine ZnS nanorods and commercial ZnS, the produced SnO<sub>2</sub>/ZnS nanocomposites exhibit 17-fold greater photostability and a 3-fold increase in photocatalytic activity. The increased separation rates of photogenerated charges, the increased number of active surface sites, and the larger light absorption range are all responsible for the improved photocatalytic performance of SnO<sub>2</sub>/ZnS nanocomposites. According to these results, SnO<sub>2</sub>/ZnS nanocomposites have a lot of potential for use as waste-water treatment photocatalysts. Table 2 provides a detailed description of recent research on the photocatalytic abilities of SnO<sub>2</sub> QD-based nanocomposites.

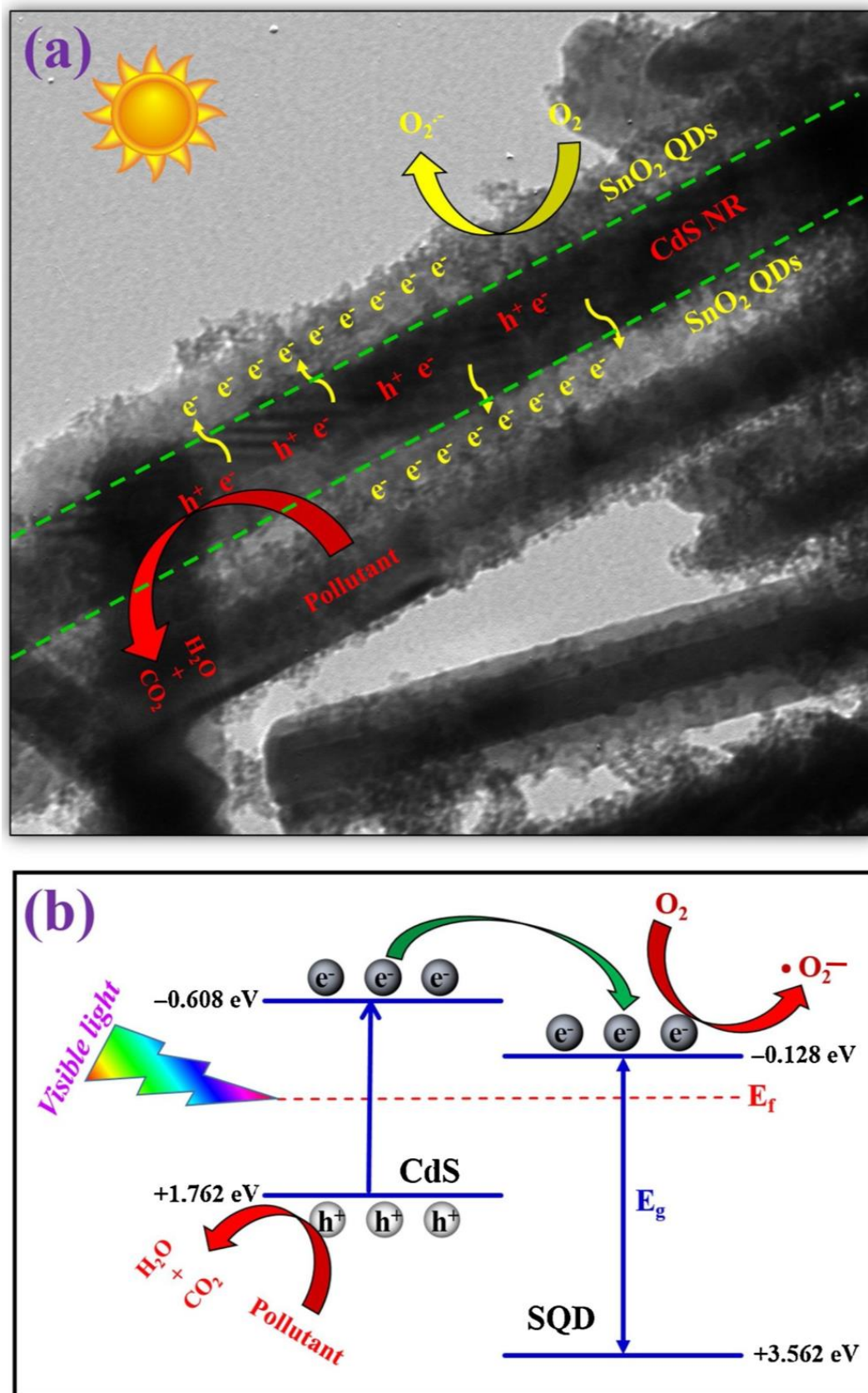


Figure 5. (a) CdS@SnO<sub>2</sub> core-shell NRs' photocatalytic degradation and (b) charge-transfer mechanism [40], Copyright 2019, Elsevier.

**Table 2.** Detailed description of recent research on the photocatalytic abilities of SnO<sub>2</sub> QD-based nanocomposites.

Photocatalyst	Bandgap	Pollutant	Dosage	Light Source	Efficiency	Stability	Ref
Au/SnO <sub>2</sub> QDs	2.71 eV	RhB	15 mg/50 mL	Visible light	98.7% in 200 min	-	[39]
Oxy-SnO <sub>2</sub> QDs	4.2 eV	Octane	-	UV-visible	91.9% in 48 h	90% after 4 cycles	[11]
Nb-SnO <sub>2</sub> QDs	2.95 eV	Polyethylene	-	Visible light	29% in 6 h	-	[51]
Ni-doped SnO <sub>2</sub> QDs	3.69 eV	RhB	-	Solar light	91.5% in 28 min	-	[44]
Ag doped SnO <sub>2</sub> QDs	3.09 eV	MB	10 mg/10 mL	Visible light	93.7% in 120 min	7 cycles	[33]
NiFe <sub>2</sub> O <sub>4</sub> /SnO <sub>2</sub>	1.754 eV	RhB	20 mg/50 mL	Visible light	98% in 105 min	93% after 3 cycles	[56]
Nb-SnO <sub>2</sub> QDs	4.74 eV	MO	30 mg/L	Visible light	99.7% in 180 min	3 cycles	[45]
Bio-SnO <sub>2</sub> QDs	3.66 eV	RhB	0.25 g/L	UV light	65% in 180 min	-	[43]
SnO <sub>2</sub> QDs/Ag <sub>3</sub> PO <sub>4</sub>	-	Carbamazepine	-	Visible light	86.5% in 120 min	66.6% in 3 cycles	[58]
Bi-doped SnO <sub>2</sub>	3.75 eV	RhB	25 mg	Sunlight	98.28% in 100 min	85.79% after 5 cycles	[46]
Ag-SnO <sub>2</sub> QDs	2.54 eV	RhB	75 mg/100 mL	Direct sunlight	98% in 180 min	4 cycles	[49]
Mn-doped SnO <sub>2</sub> QDs	1.74 eV	MO	50 mg/100 mL	Visible light	92% in 240 min	-	[48]
SnO <sub>2</sub> QDs	4.5 eV	Eosin Y	10 mg/200 mL	Direct sunlight	98% in 60 min	-	[59]
Cr-doped SnO <sub>2</sub> QDs	4.35 eV	MO	100mg/100mL	UV light	98.9% in 100 min	-	[60]
Bio-SnO <sub>2</sub> QDs	4.17 eV	Acid yellow 23	20 mg	UV light	98% in 24 min	5 cycles	[61]
SnO <sub>2</sub> -CNF	3.0 eV	Bisphenol A	50 mg /100 mL	UV light	98% in 60 min	84% after 3 cycles	[62]
Cu-doped SnO <sub>2</sub> QDs	2.4 eV	MO	100 mg/100 mL	Visible light	99% in 180 min	-	[63]

### 3.3. SnO<sub>2</sub> QDs' Integrated 2D Nanostructures

Nanocomposite heterostructures composed of various nanomaterials have demonstrated improved photocatalytic activity compared to their individual components. In particular, zero-dimensional (0D) and two-dimensional (2D) nanocomposite heterostructures exhibit great potential in photocatalysis. QDs, as a type of 0D nanocomposite, possess a high surface area-to-volume ratio, enabling efficient charge separation and transmission [64]. On the other hand, graphene-based materials, as a type of 2D nanocomposite, exhibit high electrical conductivity, excellent mechanical properties, and large surface area, leading to improved light absorption and charge transport [65]. Combining these two types of nanocomposites can achieve improved photocatalytic properties, including high efficiency, increased light absorption range, improved charge transfer, and better chemical stability. Thus, 0D and 2D nanocomposite heterostructures hold promise for various photocatalytic applications, such as water purification, air pollution control, and renewable energy conversion [66]. Due to their distinct structural and optoelectronic characteristics, two-dimensional nanocomposite heterostructures and zero-dimensional QDs are particularly appealing materials for photocatalytic applications. QDs have tunable bandgap properties and discrete energy levels, enabling efficient light absorption and exciton generation, leading to enhanced photocatalytic activity. Additionally, QDs possess a high surface area-to-volume ratio, providing a larger number of active sites for catalytic reactions. On the other hand, 2D nanocomposite heterostructures show improved photocatalytic performance as a result of their distinctive band structures and effective charge separation characteristics [67]. Increased photocatalytic efficiency results from the parting of photogenerated charge carriers being made easier by the heterojunction contact between the materials. Furthermore, 2D nanocomposite heterostructures possess large surface areas and exposed edges, providing more active sites for catalytic reactions [68]. Due to their distinct characteristics, SnO<sub>2</sub> QDs and 2D nanocomposite heterostructures are particularly interesting materials for photocatalytic applications [69]. SnO<sub>2</sub> QDs possess a high surface area-to-volume ratio, providing more active sites for chemical reactions to occur. Their small size allows for efficient light absorption and effective electron–hole pair separation. Meanwhile, SnO<sub>2</sub>/graphene and SnO<sub>2</sub>/MoS<sub>2</sub> 2D nanocomposite heterostructures exhibit enhanced photocatalytic activity due to the synergistic effect between different materials, resulting in efficient charge transfer and improved electron–hole separation [70]. Additionally, the large surface area of 2D heterostructures allows for more active sites for catalytic reactions to take place. Combining 0D SnO<sub>2</sub> QDs and 2D nanosheets in heterostructures can enhance photocatalytic activity by promoting charge separation, improving light absorption, and increasing active surface area. The unique morphology of heterostructures allows for efficient electron transport and reduced recombination of charge carriers. Therefore, creating heterostructures of 0D SnO<sub>2</sub> QDs and 2D nanosheets holds great promise for enhancing the effectiveness and selectivity of photocatalytic reactions, which might result in the creation of more effective and long-lasting environmental remediation and energy conversion processes. These initiatives are essential for tackling international problems with sustainability and renewable energy (Figure 6a–c) [71].

Babu et al. have shown that the combination of stacked g-C<sub>3</sub>N<sub>4</sub> nanolayers with SnO<sub>2</sub> QDs results in increased sunlight-driven photocatalytic activity [41]. In this study, a composite made of SnO<sub>2</sub> QDs-g-C<sub>3</sub>N<sub>4</sub> nanolayers (NLs) for reducing water pollution is synthesized and evaluated. The combination exhibits enhanced photocatalytic activity in sunshine, degrading methyl orange (MO) by 94% in about 180 min. Strong contacts between the SnO<sub>2</sub> QDs and g-C<sub>3</sub>N<sub>4</sub> NLs were seen, and the average crystallite size of the SnO<sub>2</sub> QDs was less than 3 nm. The synergistic interaction of stacked g-C<sub>3</sub>N<sub>4</sub> and SnO<sub>2</sub> QDs is responsible for the observed increase in photocatalytic activity. According to Sreekanth et al., SnO<sub>2</sub> QDs may be easily decorated in one pot on the surface of iron phosphate nanosheets for improved catalytic decolorization of methylene blue dye when NaBH<sub>4</sub> is present [72].

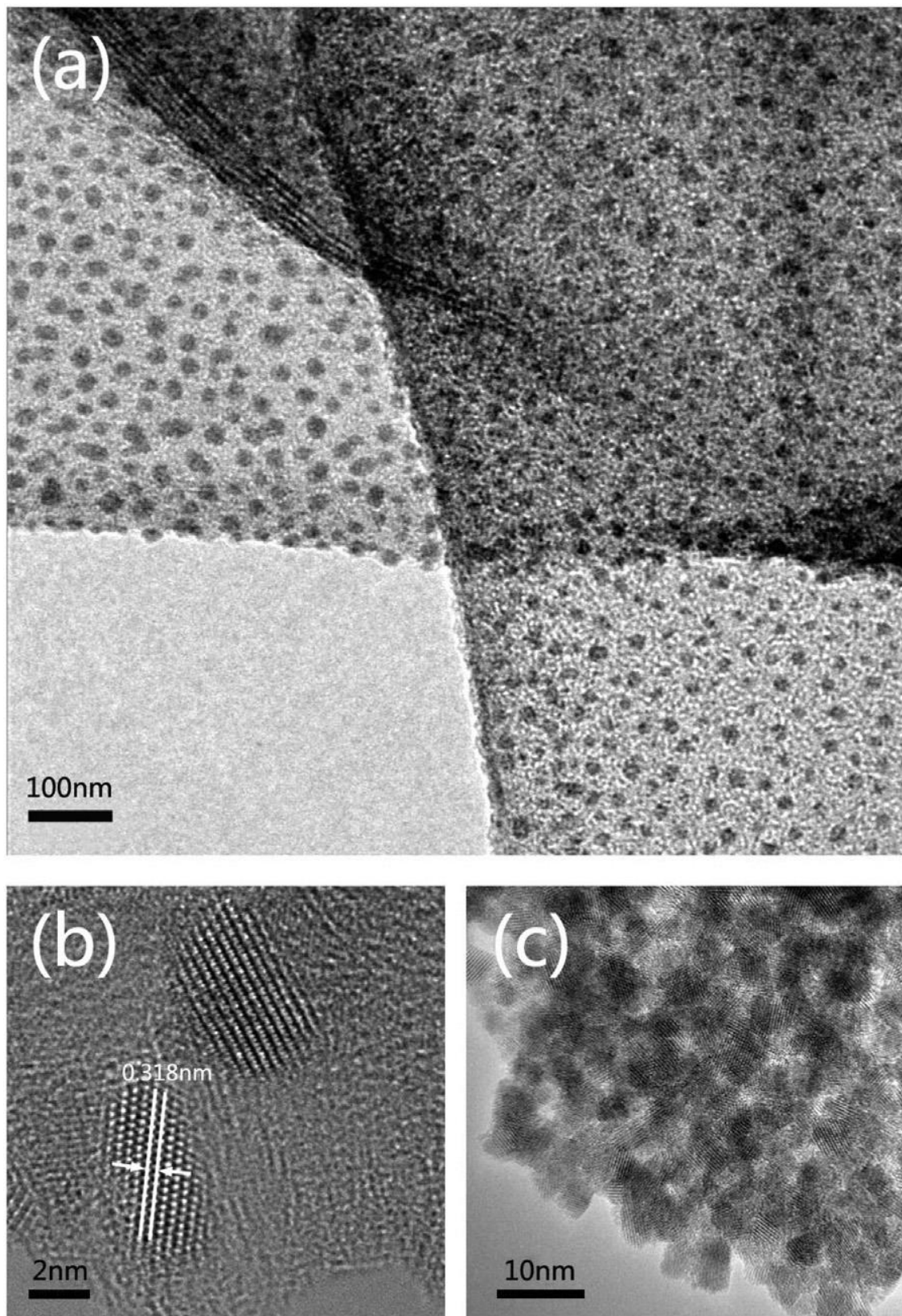


**Figure 6.** TEM images of SnO<sub>2</sub> QDs/rGO (a,b), pure SnO<sub>2</sub> QDs (c) [71], Copyright 2019, Elsevier.

The degradation of methylene blue showed increased catalytic activity in the SnO<sub>2</sub> QDs @ FePO<sub>4</sub> nanosheets nanocomposite. Bail et al. developed a novel NH<sub>3</sub> gas sensor utilizing SnO<sub>2</sub> QDs and SnS<sub>2</sub> nanosheets, as discussed in their research [73]. The authors

proposed the rational design of heterostructure as an effective method to enhance the room-temperature  $\text{NH}_3$ -sensing performance of the sensor. The  $\text{SnO}_2$  QDs/ $\text{SnS}_2$  nanocomposites were synthesized through a two-step hydrothermal method and exhibited remarkable room-temperature  $\text{NH}_3$ -sensing performance with a low detection limit of 0.1 ppm. The nanocomposites also showed good stability and reproducibility. In the study conducted by Bail et al., a new  $\text{NH}_3$  gas sensor based on  $\text{SnO}_2$  QDs and  $\text{SnS}_2$  nanosheets was introduced. The authors proposed the rational design of heterostructure as an effective means to increase the room-temperature  $\text{NH}_3$ -sensing performance of the sensor. Through a two-step hydrothermal process,  $\text{SnO}_2$  QDs/ $\text{SnS}_2$  nanocomposites were synthesized, which exhibited outstanding room-temperature  $\text{NH}_3$ -sensing performance with a low detection limit of 0.1 ppm. Furthermore, the nanocomposites demonstrated stability and reproducibility. This research report outlines the synthesis of a nanocomposite called FP-Sn, consisting of  $\text{SnO}_2$  QDs and  $\text{FePO}_4$  nanosheets (FPNSs), for the degradation of methylene blue (MB). The preparation of FP-Sn was accomplished using a simple method without any additional instruments. The catalytic efficiency of FP-Sn was improved for the degradation of MB, resulting in the successful decolorization of approximately 92% of the MB in only 6 min in the presence of  $\text{NaBH}_4$ . A unique technique for creating an integrated photocatalytic adsorbent (IPCA) was created by Mohanta et al., employing  $\text{SnO}_2$  QDs contained in carbon nanoflakes [62]. Due to the material's synergistic effect, the  $\text{SnO}_2$ -CNF nanocomposite showed improved effectiveness in the removal of bisphenol A (BPA) from water.  $\text{SnO}_2$ -CNF has a 250 mg/g Langmuir adsorption capacity, which is 1.7 and 5.3 times larger than those of bare CNF and bare  $\text{SnO}_2$ , respectively. With a removal effectiveness of about 98%, it was discovered that the coupled adsorption–photodegradation process was synergistically superior. Table 3 provides a detailed description of recent research on the photocatalytic abilities of  $\text{SnO}_2$  QD-based binary nanocomposites.

**Table 3.** Detailed description of recent research on the photocatalytic abilities of  $\text{SnO}_2$  QD-based binary nanocomposites.

Photocatalyst.	Synthesis	Pollutant	Dosage	Light Source	Efficiency	Stability	Ref
$\text{CdS}/\text{SnO}_2$	Sonochemical	RhB	-	Visible light	99% in 60 min	95% after 3 cycles	[40]
$\text{GO}/\text{SnO}_2$	Sonochemical	MB	0.5 mg/mL 250 ppm	White light	~94% in 30 min	-	[67]
$\text{SnO}_2/\text{SiO}_2$	Wet Chemical	MB	50 mg/80mL of 10 ppm	-	~100% in 5 min	4 cycles	[74]
$\text{SnO}_2/\text{g-C}_3\text{N}_4$	Solvothermal	MO	-	Sunlight	94% in 180 min	91% after 5 cycles	[41]
$\text{TiO}_2/\text{SnO}_2$	Hydrothermal	MO	100 mg/100 mL of 10 ppm	UV-visible light	99.5% in 15 min	-	[75]
$\text{SnO}_2/\text{GO}$	Sol-gel	RhB	-	Visible light	86% in 360 min	-	[76]
$\text{Ni-SnO}_2/\text{SnS}_2$	Wet chemical	MO	10 mg /50 mL of 10 ppm	solar light	92.7% in 80 min	88% after 3 cycles	[77]
$\text{g-C}_3\text{N}_4/\text{SnO}_2$	Hydrothermal	NO	200mg/15 mL of 100 ppm	Visible light	44.17% in 30 min	30% after 5 cycles	[78]
$\text{SnO}_2/\text{g-C}_3\text{N}_4$	Sonochemical	NO	400mg/15 mL of 600 ppm	Visible light	32% in 30 min	~20% after 3 cycles	[69]
$\text{SnO}_2\text{-GO}$	Solvothermal	MB	30 mg /20 mL of 10 ppm	Visible light	89.43% in 90 min	-	[79]

### 3.4. $\text{SnO}_2$ QDs in Ternary Nanocomposites

$\text{SnO}_2$  QDs have many benefits when used in ternary nanocomposites.  $\text{SnO}_2$  QDs can be coupled with other materials, such as metal oxides or carbon-based materials, to provide synergistic effects that can improve the photocatalytic activity and stability of the composite material [80]. Ternary nanocomposites are three-material structures.  $\text{SnO}_2$  QDs have a high surface-to-volume ratio and distinctive electrical characteristics that may facilitate electron transit and separation and increase photocatalytic activity.  $\text{SnO}_2$  QDs can also be used in visible-light-driven photocatalysis by changing the bandgap due to their small size. Moreover, the addition of  $\text{SnO}_2$  QDs to ternary nanocomposites can improve their stability

and durability by preventing the aggregation of other materials and safeguarding them from degradation [81].

SnO<sub>2</sub> QDs are good candidates for the development of highly effective and sustainable technologies for environmental remediation and energy conversion because they provide several advantages in ternary nanocomposites. In a study on a novel ternary nanocomposite for photocatalytic and photoelectrochemical (PEC) water-splitting applications, Babu et al. used g-C<sub>3</sub>N<sub>4</sub>, Au-SnO<sub>2</sub> QDs [82]. The three-step procedure of sonication, stirring, and annealing was used to create the ternary nanocomposite of g-CN/Au-SnO<sub>2</sub> QDs. The amount of Au-SnO<sub>2</sub> QDs loaded was tuned to increase these qualities. The inclusion of Au-SQDs into g-CN improved the light absorption and bandgap. In comparison to pure g-CN, the CNAS-20 photoelectrode demonstrated greater PEC performance with a substantially larger photocurrent. Moreover, under visible light irradiation, the ternary nanocomposite showed increased photocatalytic activity in the destruction of RhB. A higher level of photocatalytic activity resulted from the addition of SnO<sub>2</sub> QDs to the ternary nanocomposite, which facilitated electron transit and separation. A decreased charge-transfer resistance was also seen in the CNAS-20 photoelectrode, indicating improved PEC water-splitting efficiency. In order to improve solar-driven photocatalytic performance in hydrogen production and dye degradation, Ganesh et al. constructed a ternary composite comprising SnO<sub>2</sub> QDs, AgVO<sub>3</sub> nanoribbons, and g-C<sub>3</sub>N<sub>4</sub> nanosheets (0D/1D/2D) structures (Figure 7) [24]. The ternary photocatalytic system exhibited a notable improvement in photocatalytic performance for hydrogen production compared to the individual photocatalysts of g-C<sub>3</sub>N<sub>4</sub>, AgVO<sub>3</sub>, and SnO<sub>2</sub>. The ternary photocatalytic system for H<sub>2</sub> synthesis and RhB degradation under light irradiation was successfully synthesized for the investigation. During visible light irradiation, the ternary nanocomposite demonstrated enhanced photocatalytic performance for H<sub>2</sub> generation and a significant improvement in RhB degradation. Compared to the AgVO<sub>3</sub>/g-C<sub>3</sub>N<sub>4</sub> photocatalyst, the ternary nanocomposite showed improved photocatalytic activity for H<sub>2</sub> generation, which was 4.5 times higher. Furthermore, the ternary nanocomposite exhibited effective photodegradation of RhB under light irradiation in only 50 min. The removal of carbamazepine (CBZ) from the water was studied by Duan et al. using composites of Ag-SnO<sub>2</sub> QDs and silver phosphate (AgSn/AgP) [83]. With CBZ, the composites showed greater photodegradation efficiency. Superoxide, hydroxyl, and hole radicals all play a part in the mechanism underlying this improved performance. To prove that these reactive species cooperate in the breakdown of CBZ, the authors used radical trapping experiments and ESR measurements. Using liquid chromatography–mass spectrometry (LC-MS), the study discovered eight degradation intermediates. Toxicity assessments revealed that most photodegradation intermediates were less harmful than the parent drug CBZ. In order to create effective and ecologically friendly photocatalysts for eliminating organic contaminants from water, the in situ development of Ag-SnO<sub>2</sub> QDs on silver phosphate offers a potential strategy. Table 4 provides a detailed description of recent research on the photocatalytic abilities of SnO<sub>2</sub> QD-based ternary nanocomposites.

**Table 4.** Detailed description of recent research on the photocatalytic abilities of SnO<sub>2</sub> QD-based ternary nanocomposites.

Photocatalyst	Synthesis	Pollutant	Dosage	Light Source	Efficiency	Stability	Ref
g-C <sub>3</sub> N <sub>4</sub> /Au-SnO <sub>2</sub>	Sonochemical	RhB	15 mg/50 mL	Visible light	99.15% in 40 min	93.45% after 4 cycles	[82]
Au-SnO <sub>2</sub> -rGO	Hydrothermal	clothianidin	-	-	97% in 120 min	93% after 4 cycles	[84]
CQDs/SnO <sub>2-x</sub> /BiOI	Sonochemical	MO	-	LED light	91.8% in 75 min	-	[85]
SnO <sub>2</sub> /AgVO <sub>3</sub> /g-C <sub>3</sub> N <sub>4</sub>	Hydrothermal	RhB	5 mg/100 mL of 5 ppm	Visible light	84% in 50 min	~82% after 5 cycles	[24]

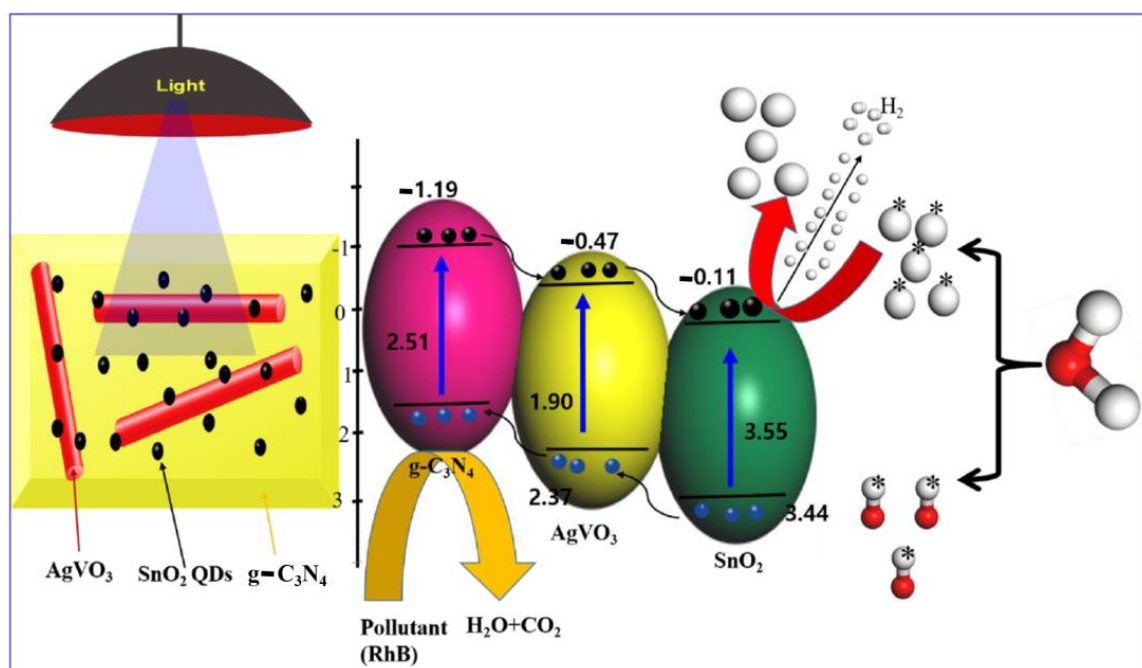


**Figure 7.** Photocatalytic mechanism of the ternary photocatalyst ( $\text{SnO}_2/\text{AgVO}_3/\text{g-C}_3\text{N}_4$ ) [24], Copyright 2019, Springer.

#### 4. Conclusions and Perspectives

In conclusion, this review article systematically presents and reviews recent advances in  $\text{SnO}_2$  quantum dot-based photocatalytic systems. Various synthesis protocols, including microwave-assisted synthesis, hydrothermal synthesis, wet chemical synthesis, chemical reduction approach, and other methods, have been discussed to synthesize  $\text{SnO}_2$  QDs. Additionally, the modification of  $\text{SnO}_2$  QDs through doping, decorating with 1D nanostructures, and integrating with 2D nanostructures and ternary nanocomposites have been thoroughly reviewed to enhance their photocatalytic performance. Based on the analysis conducted in this review article, it is evident that each synthesis method for  $\text{SnO}_2$  QDs has its own set of merits and drawbacks. This review highlights that selecting the appropriate synthesis method is crucial in determining the type of composite that can be produced with other materials, especially when doping or creating nanocomposites with other semiconductors. Additionally, it is essential to consider the morphology of other materials, such as zero-dimensional, one-dimensional, two-dimensional, or three-dimensional materials, to integrate them with  $\text{SnO}_2$  QDs effectively. The colloidal synthesis method of  $\text{SnO}_2$  QDs is most suitable for providing coverage and dispersion throughout the material when preparing one-dimensional or two-dimensional materials for nanocomposites. Conversely, when making nanocomposites with metals, such as Au, Ag, or Pd, it is preferable to use the chemical reduction method. Sol-gel, hydrothermal, and solution combustion syntheses are commonly used methods for doping purposes. While it is not possible to definitively state which synthesis method is the “best,” this review provides valuable insights to enable authors to make informed decisions about which method to use for their specific application. It is recommended that authors consider these factors when fabricating nanocomposites to obtain a better heterojunction interface for fast electron–hole charge transfer.

To enhance the photocatalytic performance of  $\text{SnO}_2$  QDs, researchers need to focus on selecting a candidate with appropriate band edge positions to create Z-scheme and S-scheme photocatalysts. Despite limited attention in this area, integrating  $\text{SnO}_2$  QDs with other materials can further improve their photocatalytic performance by forming Z-scheme and S-scheme photocatalysts. Z-scheme photocatalysts enable efficient charge separation by establishing an electron–hole transfer pathway between two different semiconductors, while S-scheme photocatalysts enhance light absorption and utilization efficiency by utiliz-

ing a cascade of energy levels between two semiconductors. Therefore, the development of SnO<sub>2</sub> QD-based Z-scheme and S-scheme photocatalysts is crucial for achieving better photocatalytic performance and promoting their practical applications in environmental remediation and energy conversion.

Ternary nanostructures incorporating SnO<sub>2</sub> QDs received less attention in previous studies. Therefore, researchers are advised to direct their focus toward this area, as it can aid in capturing more solar light. SnO<sub>2</sub> QDs possess a small size and can disperse easily in any 1D, 2D, 3D, and hierarchical nanostructures. This characteristic provides researchers with a chance to enhance the photocatalytic efficiency of SnO<sub>2</sub> QDs through the proposed approach. In addition, researchers are encouraged to explore the potential of using SnO<sub>2</sub> QDs as a protective shell material for other core materials, allowing for the maximum utilization of nanocomposites. Furthermore, researchers should focus on using SnO<sub>2</sub> QDs as the OD material in combination with 1D–2D–3D nanocomposites to achieve enhanced performance. Thus, researchers should invest in further studies to examine the efficacy of SnO<sub>2</sub> QDs in the aforementioned areas. Overall, the proposed approach will enable the development of new and improved materials that can be utilized in various applications, including energy and environmental sciences. The development of robust and durable SnO<sub>2</sub> QD-based photocatalysts can facilitate their practical application in various fields and contribute to the development of sustainable and green technologies.

**Author Contributions:** Conceptualization, methodology, validation, writing—original draft preparation, B.B.; formal analysis, resources, data curation, writing—original draft preparation, T.R.G.; writing—review and editing, supervision, J.Y.; supervision, project administration, funding acquisition, K.Y. All authors have read and agreed to the published version of the manuscript.

**Funding:** This work was supported by the National Research Foundation of Korea (NRF) grant funded by the Korean government (MSIT) (No. 2021R1C1C1011089).

**Data Availability Statement:** Not applicable.

**Conflicts of Interest:** The authors declare that they have no conflict of interest regarding the publication of this article, financial and/or otherwise.

## References

1. Sun, C.Y.; Yang, J.K.; Xu, M.; Cui, Y.; Ren, W.W.; Zhang, J.X.; Zhao, H.L.; Liang, B. Recent intensification strategies of SnO<sub>2</sub>-based photocatalysts: A review. *Chem. Eng. J.* **2022**, *427*, 131564. [[CrossRef](#)]
2. Jouyandeh, M.; Mousavi Khadem, S.S.; Habibzadeh, S.; Esmaeili, A.; Abida, O.; Vatanpour, V.; Rabiee, N.; Bagherzadeh, M.; Irvani, S.; Reza Saeb, M.; et al. Quantum dots for photocatalysis: Synthesis and environmental applications. *Green Chem.* **2021**, *23*, 4931–4954. [[CrossRef](#)]
3. Zhou, J.T.; Lyu, M.; Zhu, J.; Li, G.N.; Li, Y.T.; Jin, S.Z.; Song, J.L.; Niu, H.H.; Xu, J.Z.; Zhou, R. SnO<sub>2</sub> Quantum Dot-Modified Mesoporous TiO<sub>2</sub> Electron Transport Layer for Efficient and Stable Perovskite Solar Cells. *ACS Appl. Energy Mater.* **2022**, *5*, 3052–3063. [[CrossRef](#)]
4. Kaur, R.; Rana, A.; Singh, R.K.; Chhabra, V.A.; Kim, K.-H.; Deep, A. Efficient photocatalytic and photovoltaic applications with nanocomposites between CdTe QDs and an NTU-9 MOF. *RSC Adv.* **2017**, *7*, 29015–29024. [[CrossRef](#)]
5. Sun, P.; Xing, Z.; Li, Z.; Zhou, W. Recent advances in quantum dots photocatalysts. *Chem. Eng. J.* **2023**, *458*, 141399. [[CrossRef](#)]
6. Kumar, N.; Dagupati, R.; Lim, J.; Choi, J. Bright red luminescence from Eu<sup>3+</sup>-activated noncytotoxic SnO<sub>2</sub> quantum dots for latent fingerprint detection. *Ceram. Int.* **2022**, *48*, 17738–17748. [[CrossRef](#)]
7. Wang, Y.L.; Fan, L.Q.; Sun, S.J.; Chen, J.J.; Wu, Z.X.; Zhu, T.T.; Huang, Y.F.; Wu, J.H. Ti<sub>3</sub>C<sub>2</sub>T<sub>x</sub> MXene supported SnO<sub>2</sub> quantum dots with oxygen vacancies as anode for Li-ion capacitors. *Chem. Eng. J.* **2022**, *428*, 131993. [[CrossRef](#)]
8. Chen, D.Y.; Huang, S.S.; Huang, R.T.; Zhang, Q.; Le, T.T.; Cheng, E.B.; Hu, Z.J.; Chen, Z.W. Highlights on advances in SnO<sub>2</sub> quantum dots: Insights into synthesis strategies, modifications and applications. *Mater. Res. Lett.* **2018**, *6*, 462–488. [[CrossRef](#)]
9. Wu, T.T.; Zhen, C.; Wu, J.B.; Jia, C.X.; Haider, M.; Wang, L.Z.; Liu, G.; Cheng, H.M. Chlorine capped SnO<sub>2</sub> quantum-dots modified TiO<sub>2</sub> electron selective layer to enhance the performance of planar perovskite solar cells. *Sci. Bull.* **2019**, *64*, 547–552. [[CrossRef](#)]
10. Xu, Y.; Matios, E.; Luo, J.M.; Li, T.; Lu, X.; Jiang, S.H.; Yue, Q.; Li, W.Y.; Kang, Y.J. SnO<sub>2</sub> Quantum Dots Enabled Site-Directed Sodium Deposition for Stable Sodium Metal Batteries. *Nano Lett.* **2021**, *21*, 816–822. [[CrossRef](#)]

11. Liu, J.Q.; Zhang, Q.R.; Tian, X.Y.; Hong, Y.; Nie, Y.C.; Su, N.N.; Jin, G.H.; Zhai, Z.X.; Fu, C. Highly efficient photocatalytic degradation of oil pollutants by oxygen deficient SnO<sub>2</sub> quantum dots for water remediation. *Chem. Eng. J.* **2021**, *404*, 127146. [[CrossRef](#)]
12. Sahu, B.K.; Kaur, G.; Das, A. Revealing Interplay of Defects in SnO<sub>2</sub> Quantum Dots for Blue Luminescence and Selective Trace Ammonia Detection at Room Temperature. *ACS Appl. Mater. Interfaces* **2020**, *12*, 49227–49236. [[CrossRef](#)]
13. Han, X.; Zhao, J.J.; An, L.; Li, Z.H.; Yu, X. One-step synthesis of oxygen vacancy-rich SnO<sub>2</sub> quantum dots with ultrahigh visible-light photocatalytic activity. *Mater. Res. Bull.* **2019**, *118*, 110486. [[CrossRef](#)]
14. Das, J.; Dhar, S.S. Synthesis of SnO<sub>2</sub> quantum dots mediated by *Camellia sinensis* shoots for degradation of thiamethoxam. *Toxicol. Environ. Chem.* **2020**, *102*, 186–196. [[CrossRef](#)]
15. Bhawna; Kumar, S.; Sharma, R.; Gupta, A.; Tyagi, A.; Singh, P.; Kumar, A.; Kumar, V. Recent insights into SnO<sub>2</sub>-based engineered nanoparticles for sustainable H-2 generation and remediation of pesticides. *New J. Chem.* **2022**, *46*, 4014–4048. [[CrossRef](#)]
16. Wu, Z.D.; Jing, H.Y.; Zhao, Y.; Lu, K.R.; Liu, B.Y.; Yu, J.; Xia, X.F.; Lei, W.; Hao, Q.L. Grain boundary and interface interaction Co-regulation promotes SnO<sub>2</sub> quantum dots for efficient CO<sub>2</sub> reduction. *Chem. Eng. J.* **2023**, *451*, 138477. [[CrossRef](#)]
17. Sun, B.; Chen, Y.Z.; Tao, L.; Zhao, H.B.; Zhou, G.D.; Xia, Y.D.; Wang, H.Y.; Zhao, Y. Nanorod Array of SnO<sub>2</sub> Quantum Dot Interspersed Multiphase TiO<sub>2</sub> Heterojunctions with Highly Photocatalytic Water Splitting and Self-Rechargeable Battery-Like Applications. *ACS Appl. Mater. Interfaces* **2019**, *11*, 2071–2081. [[CrossRef](#)]
18. Mallikarjuna, K.; Rafiqul Bari, G.A.K.M.; Vattikuti, S.V.P.; Kim, H. Synthesis of carbon-doped SnO<sub>2</sub> nanostructures for visible-light-driven photocatalytic hydrogen production from water splitting. *Int. J. Hydrogen Energy* **2020**, *45*, 32789–32796. [[CrossRef](#)]
19. Sheikh, S.P.; Reddy, V.R.; Sen, P. Size-dependent nonlinear optical absorption in SnO<sub>2</sub> quantum dots. *J. Opt. Soc. Am. B-Opt. Phys.* **2020**, *37*, 2788–2795. [[CrossRef](#)]
20. Liu, J.Q.; Nie, Y.C.; Xue, W.T.; Wu, L.T.; Jin, H.; Jin, G.H.; Zhai, Z.X.; Fu, C. Size effects on structural and optical properties of tin oxide quantum dots with enhanced quantum confinement. *J. Mater. Res. Technol.-JMRT* **2020**, *9*, 8020–8028. [[CrossRef](#)]
21. Mishra, S.R.; Ahmaruzzaman, M. Tin oxide based nanostructured materials: Synthesis and potential applications. *Nanoscale* **2022**, *14*, 1566–1605. [[CrossRef](#)]
22. Jin, W.; Wang, H.; Liu, Y.L.; Yang, S.; Zhou, J.; Chen, W. SnO<sub>2</sub> Quantum Dots-Functionalized MoO<sub>3</sub> Nanobelts for High-Selectivity Ethylene Sensing. *ACS Appl. Nano Mater.* **2022**, *5*, 10485–10494. [[CrossRef](#)]
23. Lee, J.H.; Mirzaei, A.; Kim, J.H.; Kim, J.Y.; Nasriddinov, A.F.; Rummyantseva, M.N.; Kim, H.W.; Kim, S.S. Gas-sensing behaviors of TiO<sub>2</sub>-layer-modified SnO<sub>2</sub> quantum dots in self-heating mode and effects of the TiO<sub>2</sub> layer. *Sens. Actuator B-Chem.* **2020**, *310*, 127870. [[CrossRef](#)]
24. Koyyada, G.; Kumar, N.S.; Al-Ghurabi, E.H.; Asif, M.; Mallikarjuna, K. Enhanced solar-driven photocatalytic performance of a ternary composite of SnO<sub>2</sub> quantum dots//AgVO<sub>3</sub> nanoribbons//g-C<sub>3</sub>N<sub>4</sub> nanosheets (0D/1D/2D) structures for hydrogen production and dye degradation. *Environ. Sci. Pollut. Res.* **2021**, *28*, 31585–31595. [[CrossRef](#)] [[PubMed](#)]
25. Praveen, S.; Veeralingam, S.; Badhulika, S. A Flexible Self-Powered UV Photodetector and Optical UV Filter Based on beta-Bi<sub>2</sub>O<sub>3</sub>/SnO<sub>2</sub> Quantum Dots Schottky Heterojunction. *Adv. Mater. Interfaces* **2021**, *8*, 2100373. [[CrossRef](#)]
26. Xu, Z.J.; Jiang, Y.; Li, Z.X.; Chen, C.; Kong, X.Y.; Chen, Y.W.; Zhou, G.F.; Liu, J.M.; Kempa, K.; Gao, J.W. Rapid Microwave-Assisted Synthesis of SnO<sub>2</sub> Quantum Dots for Efficient Planar Perovskite Solar Cells. *ACS Appl. Energy Mater.* **2021**, *4*, 1887–1893. [[CrossRef](#)]
27. Liu, H.R.; Chen, Z.L.; Wang, H.B.; Ye, F.H.; Ma, J.J.; Zheng, X.L.; Gui, P.B.; Xiong, L.B.; Wen, J.; Fang, G.J. A facile room temperature solution synthesis of SnO<sub>2</sub> quantum dots for perovskite solar cells. *J. Mater. Chem. A* **2019**, *7*, 10636–10643. [[CrossRef](#)]
28. Dutta, D.; Bahadur, D. Influence of confinement regimes on magnetic property of pristine SnO<sub>2</sub> quantum dots. *J. Mater. Chem.* **2012**, *22*, 24545–24551. [[CrossRef](#)]
29. Manikandan, D.; Yadav, A.K.; Jha, S.N.; Bhattacharyya, D.; Boukhvalov, D.W.; Murugan, R. XANES, EXAFS, EPR, and First-Principles Modeling on Electronic Structure and Ferromagnetism in Mn Doped SnO<sub>2</sub> Quantum Dots. *J. Phys. Chem. C* **2019**, *123*, 3067–3075. [[CrossRef](#)]
30. do Nascimento, J.L.A.; Chantelle, L.; dos Santos, I.M.G.; de Oliveira, A.L.M.; Alves, M.C.F. The Influence of Synthesis Methods and Experimental Conditions on the Photocatalytic Properties of SnO<sub>2</sub>: A Review. *Catalysts* **2022**, *12*, 428. [[CrossRef](#)]
31. Zhao, X.X.; Yang, Q.; Quan, Z.W. Tin-based nanomaterials: Colloidal synthesis and battery applications. *Chem. Commun.* **2019**, *55*, 8683–8694. [[CrossRef](#)] [[PubMed](#)]
32. Geng, J.G.; Ma, C.T.; Zhang, D.; Ning, X.F. Facile and fast synthesis of SnO<sub>2</sub> quantum dots for high performance solid-state asymmetric supercapacitor. *J. Alloys Compd.* **2020**, *825*, 153850. [[CrossRef](#)]
33. Parthibavarman, M.; Sathishkumar, S.; Jayashree, M.; BoopathiRaja, R. Microwave Assisted Synthesis of Pure and Ag Doped SnO<sub>2</sub> Quantum Dots as Novel Platform for High Photocatalytic Activity Performance. *J. Clust. Sci.* **2019**, *30*, 351–363. [[CrossRef](#)]
34. Yu, B.; Li, Y.C.; Wang, Y.J.; Li, H.; Zhang, R.P. Facile hydrothermal synthesis of SnO<sub>2</sub> quantum dots with enhanced photocatalytic degradation activity: Role of surface modification with chloroacetic acid. *J. Environ. Chem. Eng.* **2021**, *9*, 105618. [[CrossRef](#)]
35. Cheng, Y.; Wang, S.H.; Zhou, L.; Chang, L.M.; Liu, W.Q.; Yin, D.M.; Yi, Z.; Wang, L.M. SnO<sub>2</sub> Quantum Dots: Rational Design to Achieve Highly Reversible Conversion Reaction and Stable Capacities for Lithium and Sodium Storage. *Small* **2020**, *16*, e2000681. [[CrossRef](#)]
36. Gao, L.; Wu, G.S.; Ma, J.; Jiang, T.C.; Chang, B.; Huang, Y.S.; Han, S. SnO<sub>2</sub> Quantum Dots@Graphene Framework as a High-Performance Flexible Anode Electrode for Lithium-Ion Batteries. *ACS Appl. Mater. Interfaces* **2020**, *12*, 12982–12989. [[CrossRef](#)]

37. Chen, M.Y.; Chen, X.T.; Ma, W.C.; Sun, X.J.; Wu, L.J.; Lin, X.F.; Yang, Y.X.; Li, R.; Shen, D.Y.; Chen, Y.; et al. Highly Stable SnO<sub>2</sub>-Based Quantum-Dot Light-Emitting Diodes with the Conventional Device Structure. *ACS Nano* **2022**, *16*, 9631–9639. [[CrossRef](#)]
38. Huang, Q.Q.; Liao, J.Y.; Zhang, Q.Y.; Lai, N.; Zhang, B.W.; Wang, C.; Yang, J.; Yang, Y.; Wang, J.; Zhang, G.L.; et al. The synergistic effect of lead-free quantum dots and SnO<sub>2</sub> in glass-ceramics for broadband white-emission. *J. Mater. Chem. C* **2022**, *10*, 18285–18293. [[CrossRef](#)]
39. Babu, B.; Koutavarapu, R.; Harish, V.V.N.; Shim, J.; Yoo, K. Novel in-situ synthesis of Au/SnO<sub>2</sub> quantum dots for enhanced visible-light-driven photocatalytic applications. *Ceram. Int.* **2019**, *45*, 5743–5750. [[CrossRef](#)]
40. Babu, B.; Harish, V.V.N.; Koutavarapu, R.; Shim, J.; Yoo, K. Enhanced visible-light-active photocatalytic performance using CdS nanorods decorated with colloidal SnO<sub>2</sub> quantum dots: Optimization of core-shell nanostructure. *J. Ind. Eng. Chem.* **2019**, *76*, 476–487. [[CrossRef](#)]
41. Babu, B.; Cho, M.; Byon, C.; Shim, J. Sunlight-driven photocatalytic activity of SnO<sub>2</sub> QDs-g-C<sub>3</sub>N<sub>4</sub> nanolayers. *Mater. Lett.* **2018**, *212*, 327–331. [[CrossRef](#)]
42. Wahab, R.; Khan, F.; Al-Khedhairi, A.A. Quantization of SnO<sub>2</sub> dots: Apoptosis and intrinsic effect of quantum dots for myoblast cancer cells with caspase 3/7 genes. *Ceram. Int.* **2020**, *46*, 6383–6395. [[CrossRef](#)]
43. Fatimah, I.; Sahroni, I.; Muraza, O.; Doong, R.A. One-pot biosynthesis of SnO<sub>2</sub> quantum dots mediated by Clitoria ternatea flower extract for photocatalytic degradation of rhodamine B. *J. Environ. Chem. Eng.* **2020**, *8*, 103879. [[CrossRef](#)]
44. Chen, D.Y.; Huang, S.S.; Huang, R.T.; Zhang, Q.; Le, T.T.; Cheng, E.B.; Hu, Z.J.; Chen, Z.W. Convenient fabrication of Ni-doped SnO<sub>2</sub> quantum dots with improved photodegradation performance for Rhodamine B. *J. Alloys Compd.* **2019**, *788*, 929–935. [[CrossRef](#)]
45. Wang, Y.; Su, N.N.; Liu, J.Q.; Lin, Y.H.; Wang, J.K.; Guo, X.; Zhang, Y.H.; Qin, Z.K.; Liu, J.F.; Zhang, C.Y.; et al. Enhanced visible-light photocatalytic properties of SnO<sub>2</sub> quantum dots by niobium modification. *Results Phys.* **2022**, *37*, 105515. [[CrossRef](#)]
46. Chu, L.L.; Duo, F.F.; Zhang, M.L.; Wu, Z.S.; Sun, Y.Y.; Wang, C.; Dong, S.Y.; Sun, J.H. Doping induced enhanced photocatalytic performance of SnO<sub>2</sub>:Bi<sup>3+</sup> quantum dots toward organic pollutants. *Colloid Surf. A-Physicochem. Eng. Asp.* **2020**, *589*, 124416. [[CrossRef](#)]
47. Zhu, L.F.; Wang, M.Y.; Lam, T.K.; Zhang, C.Y.; Du, H.D.; Li, B.H.; Yao, Y.W. Fast microwave-assisted synthesis of gas-sensing SnO<sub>2</sub> quantum dots with high sensitivity. *Sens. Actuator B-Chem.* **2016**, *236*, 646–653. [[CrossRef](#)]
48. Babu, B.; Kadam, A.N.; Rao, G.T.; Lee, S.W.; Byon, C.; Shim, J. Enhancement of visible-light-driven photoresponse of Mn-doped SnO<sub>2</sub> quantum dots obtained by rapid and energy efficient synthesis. *J. Lumin.* **2018**, *195*, 283–289. [[CrossRef](#)]
49. Babu, B.; Cho, M.Y.; Byon, C.; Shim, J. One pot synthesis of Ag-SnO<sub>2</sub> quantum dots for highly enhanced sunlight-driven photocatalytic activity. *J. Alloys Compd.* **2018**, *731*, 162–171. [[CrossRef](#)]
50. Kaur, H.; Bhatti, H.S.; Singh, K. Dopant incorporation in ultrasmall quantum dots: A case study on the effect of dopant concentration on lattice and properties of SnO<sub>2</sub> QDs. *J. Mater. Sci.-Mater. Electron.* **2019**, *30*, 2246–2264. [[CrossRef](#)]
51. Shao, J.; Deng, K.; Chen, L.; Guo, C.M.; Zhao, C.S.; Cui, J.Y.; Shen, T.A.; Li, K.W.; Liu, J.Q.; Fu, C. Aqueous synthesis of Nb-modified SnO<sub>2</sub> quantum dots for efficient photocatalytic degradation of polyethylene for in situ agricultural waste treatment. *Green Process. Synth.* **2021**, *10*, 499–506. [[CrossRef](#)]
52. Wu, C.P.; Xie, K.X.; He, J.P.; Wang, Q.P.; Ma, J.M.; Yang, S.; Wang, Q.H. SnO<sub>2</sub> quantum dots modified N-doped carbon as high-performance anode for lithium ion batteries by enhanced pseudocapacitance. *Rare Met.* **2021**, *40*, 48–56. [[CrossRef](#)]
53. Fan, D.W.; Liu, X.; Shao, X.R.; Zhang, Y.; Zhang, N.; Wang, X.Y.; Wei, Q.; Ju, H.X. A cardiac troponin I photoelectrochemical immunosensor: Nitrogen-doped carbon quantum dots-bismuth oxyiodide-flower-like SnO<sub>2</sub>. *Microchim. Acta* **2020**, *187*, 332. [[CrossRef](#)]
54. Liu, Y.; Wei, S.; Wang, G.; Tong, J.Y.; Li, J.; Pan, D.C. Quantum-Sized SnO<sub>2</sub> Nanoparticles with Upshifted Conduction Band: A Promising Electron Transportation Material for Quantum Dot Light-Emitting Diodes. *Langmuir* **2020**, *36*, 6605–6609. [[CrossRef](#)] [[PubMed](#)]
55. Liu, D.; Li, Y.; Zhang, X.L.; Yang, L.; Luo, X. Heterostructured Perylene Diimide (PDI) Supramolecular Nanorods with SnO<sub>2</sub> Quantum Dots for Enhanced Visible-Light Photocatalytic Activity and Stability. *ChemCatChem* **2022**, *14*, e202200087. [[CrossRef](#)]
56. Babu, B.; Koutavarapu, R.; Shim, J.; Yoo, K. SnO<sub>2</sub> quantum dots decorated NiFe<sub>2</sub>O<sub>4</sub> nanoplates: 0D/2D heterojunction for enhanced visible-light-driven photocatalysis. *Mater. Sci. Semicond. Process* **2020**, *107*, 104834. [[CrossRef](#)]
57. Hui, W.; Yang, Y.G.; Xu, Q.; Gu, H.; Feng, S.L.; Su, Z.H.; Zhang, M.R.; Wang, J.O.; Li, X.D.; Fang, J.F.; et al. Red-Carbon-Quantum-Dot-Doped SnO<sub>2</sub> Composite with Enhanced Electron Mobility for Efficient and Stable Perovskite Solar Cells. *Adv. Mater.* **2020**, *32*, e1906374. [[CrossRef](#)]
58. Duan, Z.R.; Deng, L.; Shi, Z.; Zhang, H.J.; Zeng, H.X.; Crittenden, J. In situ growth of Ag-SnO<sub>2</sub> quantum dots on silver phosphate for photocatalytic degradation of carbamazepine: Performance, mechanism and intermediates toxicity assessment. *J. Colloid Interface Sci.* **2019**, *534*, 270–278. [[CrossRef](#)]
59. Bhattacharjee, A.; Ahmaruzzaman, M. Facile synthesis of SnO<sub>2</sub> quantum dots and its photocatalytic activity in the degradation of eosin Y dye: A green approach. *Mater. Lett.* **2015**, *139*, 418–421. [[CrossRef](#)]
60. Reddy, C.V.; Babu, B.; Shim, J. Synthesis of Cr-doped SnO<sub>2</sub> quantum dots and its enhanced photocatalytic activity. *Mater. Sci. Eng. B-Adv. Funct. Solid-State Mater.* **2017**, *223*, 131–142. [[CrossRef](#)]

61. Begum, S.; Ahmaruzzaman, M. Green synthesis of SnO<sub>2</sub> quantum dots using *Parkia speciosa* Hassk pods extract for the evaluation of anti-oxidant and photocatalytic properties. *J. Photochem. Photobiol. B-Biol.* **2018**, *184*, 44–53. [[CrossRef](#)]
62. Mohanta, D.; Ahmaruzzaman, M. Biogenic synthesis of SnO<sub>2</sub> quantum dots encapsulated carbon nanoflakes: An efficient integrated photocatalytic adsorbent for the removal of bisphenol A from aqueous solution. *J. Alloys Compd.* **2020**, *828*, 154093. [[CrossRef](#)]
63. Babu, B.; Kadam, A.N.; Ravikumar, R.; Byon, C. Enhanced visible light photocatalytic activity of Cu-doped SnO<sub>2</sub> quantum dots by solution combustion synthesis. *J. Alloys Compd.* **2017**, *703*, 330–336. [[CrossRef](#)]
64. Ren, W.W.; Yang, J.K.; Zhang, J.X.; Li, W.; Sun, C.Y.; Zhao, H.L.; Wen, Y.T.; Sha, O.; Liang, B. Recent progress in SnO<sub>2</sub>/g-C<sub>3</sub>N<sub>4</sub> heterojunction photocatalysts: Synthesis, modification, and application. *J. Alloys Compd.* **2022**, *906*, 164372. [[CrossRef](#)]
65. Wei, Z.P.; Liu, M.N.; Li, H.G.; Sun, S.S.; Yang, L.Y. SnO<sub>2</sub> Quantum Dots Decorated Reduced Graphene Oxide Nanosheets Composites for Electrochemical Supercapacitor Applications. *Int. J. Electrochem. Sci.* **2020**, *15*, 6257–6268. [[CrossRef](#)]
66. Sharma, I.; Kumar, K.N.; Choi, J. Highly sensitive chemiresistive detection of NH<sub>3</sub> by formation of WS<sub>2</sub> nanosheets and SnO<sub>2</sub> quantum dot heterostructures. *Sens. Actuator B-Chem.* **2023**, *375*, 132899. [[CrossRef](#)]
67. Sahu, B.K.; Juine, R.N.; Sahoo, M.; Kumar, R.; Das, A. Interface of GO with SnO<sub>2</sub> quantum dots as an efficient visible-light photocatalyst. *Chemosphere* **2021**, *276*, 130142. [[CrossRef](#)]
68. Shao, S.F.; Chen, X.; Chen, Y.Y.; Zhang, L.; Kim, H.W.; Kim, S.S. ZnO Nanosheets Modified with Graphene Quantum Dots and SnO<sub>2</sub> Quantum Nanoparticles for Room-Temperature H<sub>2</sub>S Sensing. *ACS Appl. Nano Mater.* **2020**, *3*, 5220–5230. [[CrossRef](#)]
69. Zou, Y.Z.; Xie, Y.; Yu, S.; Chen, L.; Cui, W.; Dong, F.; Zhou, Y. SnO<sub>2</sub> quantum dots anchored on g-C<sub>3</sub>N<sub>4</sub> for enhanced visible-light photocatalytic removal of NO and toxic NO<sub>2</sub> inhibition. *Appl. Surf. Sci.* **2019**, *496*, 143630. [[CrossRef](#)]
70. Luo, J.T.; Li, C.; Yang, Q.T.; Yan, L.X.; Zhang, B.H.; Tao, R.; Rauf, S.; Li, H.L.; Fu, C. Facile Fabrication of MoS<sub>2</sub> Nanoflowers/SnO<sub>2</sub> Colloidal Quantum Dots Nanocomposite for Enhanced NO<sub>2</sub> Sensing at Room Temperature. *IEEE Sens. J.* **2022**, *22*, 6295–6302. [[CrossRef](#)]
71. Ren, L.; Yao, Y.; Wang, K.Y.; Li, S.T.; Zhu, K.J.; Liu, J. Novel one-step in situ growth of SnO<sub>2</sub> quantum dots on reduced graphene oxide and its application for lithium ion batteries. *J. Solid State Chem.* **2019**, *273*, 128–131. [[CrossRef](#)]
72. Sreekanth, T.V.M.; Ramaraghavulu, R.; Yoo, K.; Kim, J. Facile One-Pot Decoration of SnO<sub>2</sub> Quantum Dots on the Surface of the Iron Phosphate Nanosheets for Enhanced Catalytic Decolorization of Methylene Blue Dye in the Presence of NaBH<sub>4</sub>. *J. Clust. Sci.* **2022**, *33*, 835–838. [[CrossRef](#)]
73. Bai, J.Z.; Shen, Y.B.; Zhao, S.K.; Chen, Y.S.; Li, G.D.; Han, C.; Wei, D.Z.; Yuan, Z.Y.; Meng, F.L. Flower-like MoS<sub>2</sub> hierarchical architectures assembled by 2D nanosheets sensitized with SnO<sub>2</sub> quantum dots for high-performance NH<sub>3</sub> sensing at room temperature. *Sens. Actuator B-Chem.* **2022**, *353*, 131191. [[CrossRef](#)]
74. Dutta, D.; Thakur, D.; Bahadur, D. SnO<sub>2</sub> quantum dots decorated silica nanoparticles for fast removal of cationic dye (methylene blue) from wastewater. *Chem. Eng. J.* **2015**, *281*, 482–490. [[CrossRef](#)]
75. Du, F.; Zuo, X.; Yang, Q.; Yang, B.; Li, G.; Ding, Z.; Wu, M.; Ma, Y.; Jin, S.; Zhu, K. Facile assembly of TiO<sub>2</sub> nanospheres/SnO<sub>2</sub> quantum dots composites with excellent photocatalyst activity for the degradation of methyl orange. *Ceram. Int.* **2016**, *42*, 12778–12782. [[CrossRef](#)]
76. Tajima, T.; Goto, H.; Nishi, M.; Ohkubo, T.; Nishina, Y.; Miyake, H.; Takaguchi, Y. A facile synthesis of a SnO<sub>2</sub>/Graphene oxide nano-nano composite and its photoreactivity. *Mater. Chem. Phys.* **2018**, *212*, 149–154. [[CrossRef](#)]
77. Chen, D.; Huang, S.; Huang, R.; Zhang, Q.; Le, T.-T.; Cheng, E.; Yue, R.; Hu, Z.; Chen, Z. Construction of Ni-doped SnO<sub>2</sub>-SnS<sub>2</sub> heterojunctions with synergistic effect for enhanced photodegradation activity. *J. Hazard. Mater.* **2019**, *368*, 204–213. [[CrossRef](#)] [[PubMed](#)]
78. Van Pham, V.; Mai, D.-Q.; Bui, D.-P.; Van Man, T.; Zhu, B.; Zhang, L.; Sangkaworn, J.; Tantirungrotechai, J.; Reutrakul, V.; Cao, T.M. Emerging 2D/0D g-C<sub>3</sub>N<sub>4</sub>/SnO<sub>2</sub> S-scheme photocatalyst: New generation architectural structure of heterojunctions toward visible-light-driven NO degradation. *Environ. Pollut.* **2021**, *286*, 117510. [[CrossRef](#)]
79. Fu, Z.; Qin, B.; Guo, X.; Wang, Y.; Xu, Y.; Qiao, Q.; Wang, Q.; Wang, F.; Gao, S.; Yang, Z. Enhancement of photocatalytic dye degradation and photoconversion capacity of graphene oxide/SnO<sub>2</sub> nanocomposites. *J. Alloys Compd.* **2022**, *898*, 162796. [[CrossRef](#)]
80. Niu, J.J.; Pan, J.Q.; Fu, W.D.; Xiao, G.S.; Fu, Y.Y.; Cao, J.; Wang, J.J.; Zheng, Y.Y.; Shi, L.; Li, C.R. The photovoltaic enhancement of Cu<sub>2</sub>O/SnO<sub>2</sub> quantum dots/ZnO arrays transparent pn junction device via carrier injection and potential transition of SiO<sub>2</sub> QDs. *J. Mater. Sci.-Mater. Electron.* **2022**, *33*, 7300–7311. [[CrossRef](#)]
81. Zhu, J.K.; Li, H.; Cui, X.Q.; Yang, Z.Y.; Chen, B.; Li, Y.H.; Zhang, P.F.; Li, J.R. Efficient photocathodic protection performance of ZnIn<sub>2</sub>S<sub>4</sub> nanosheets/SnO<sub>2</sub> quantum dots/TiO<sub>2</sub> nanotubes composite for 316 SS under visible light. *J. Alloys Compd.* **2022**, *926*, 166901. [[CrossRef](#)]
82. Babu, B.; Koutavarapu, R.; Shim, J.; Yoo, K. Enhanced visible-light-driven photoelectrochemical and photocatalytic performance of Au-SnO<sub>2</sub> quantum dot-anchored g-C<sub>3</sub>N<sub>4</sub> nanosheets. *Sep. Purif. Technol.* **2020**, *240*, 116652. [[CrossRef](#)]
83. Chen, Y.W.; Jiang, Y.F.; Chen, B.Y.; Ye, F.L.; Duan, H.Q.; Cui, H.Y. Facile fabrication of N-doped carbon quantum dots modified SnO<sub>2</sub> composites for improved visible light photocatalytic activity. *Vacuum* **2021**, *191*, 110371. [[CrossRef](#)]

84. Mohanta, D.; Ahmaruzzaman, M. A novel Au-SnO<sub>2</sub>-rGO ternary nanoheterojunction catalyst for UV-LED induced photocatalytic degradation of clothianidin: Identification of reactive intermediates, degradation pathway and in-depth mechanistic insight. *J. Hazard. Mater.* **2020**, *397*, 122685. [[CrossRef](#)] [[PubMed](#)]
85. Song, Z.; Wang, C.; Shu, S.; Liu, J.; Liu, J.; Li, Y.; Huang, L.; Huang, L. Facile synthesis CQDs/SnO<sub>2-x</sub>/BiOI heterojunction photocatalyst to effectively degrade pollutants and antibacterial under LED light. *J. Photochem. Photobiol. B Biol.* **2022**, *236*, 112566. [[CrossRef](#)] [[PubMed](#)]

**Disclaimer/Publisher's Note:** The statements, opinions and data contained in all publications are solely those of the individual author(s) and contributor(s) and not of MDPI and/or the editor(s). MDPI and/or the editor(s) disclaim responsibility for any injury to people or property resulting from any ideas, methods, instructions or products referred to in the content.